Precambrian Research 165 (2008) 243–259

Contents lists available at ScienceDirect

Precambrian Research

journal homepage: www.elsevier.com/locate/precamres

Stratigraphic relationships of Cryogenian strata disconformably overlying the Bitter Springs Formation, northeastern Amadeus Basin, Central Australia

Steven J. Skotnicki[a,*], Andrew C. Hill[b], Malcolm Walter[c], Richard Jenkins[d]

[a] 281 West Amoroso Drive, Gilbert, AZ 85233, USA
[b] Centro de Astrobiología (INTA-CSIC), Instituto Nacional de Técnica Aeroespacial, Ctra de Ajalvir, km 4, 28850 Torrejón de Ardoz, Madrid, Spain
[c] Australian Centre for Astrobiology, School of Biotechnology and Biomolecular Sciences, University of New South Wales, Kensington, NSW, Australia
[d] South Australian Museum, Adelaida, SA 5000, Australia

ARTICLE INFO

Article history:
Received 19 September 2007
Received in revised form 21 June 2008
Accepted 27 June 2008

Keywords:
Neoproterozoic
Amadeus Basin
Bitter Springs Formation
Paleokarst
C stable isotopes
O stable isotopes

ABSTRACT

Detailed mapping and C and O stable isotopic data from sedimentary carbonate in units both above and below the paleo-erosion surface on the Bitter Springs Formation (BSF) in the northeastern Amadeus Basin, Australia, have clarified the stratigraphy of the area. Isotopic data indicate that the top of the Loves Creek Member of the Bitter Springs Formation is preserved near Corroboree Rock, and is overlain by fenestrate-carbonate-clast breccia, and dolomitic quartz sandstone and chert-pebble conglomerate of the Pioneer Sandstone. The isotopic data, as well as lithologic data, indicate the presence of a 1–2 m-thick cap carbonate preserved between Corroboree Rock and areas 10 km to the northeast. In many places the cap carbonate layer is mostly a syn-sedimentary dolomite-clast breccia, consistent with deposition and disturbance in shallow water. C and O isotopic data also indicate that thin-bedded sandstone and dolomite above the Bitter Springs Formation at Ellery Creek, and a newly discovered massive chert-bearing dolomite at Ross River could both belong to the glaciogenic Olympic Formation. Detailed mapping also provides a more detailed context for the famous black chert microfossil locality in the Bitter Springs Formation at Ross River.

1. Introduction

The original goal of this project was to examine the top of the Bitter Springs Formation (BSF) in the Amadeus Basin for evidence of karsting and to search for evidence of land life that may have existed on the karst surface during the Neoproterozoic. Previous workers (Preiss et al., 1978) described significant paleotopography and deep channels in the BSF west of Ellery Creek, and well-exposed karst features at the top of the formation between the Mulga and Gaylad synclines (Freeman et al., 1991). Southgate (1991) described desiccation cracks, meniscus and pendant cements in grainstones, indurated erosion surfaces, and karst associated with subaerial exposure during deposition of several of the thinly bedded dolostone units. Froelich and Krieg (1969) described solution collapse structures (solution breccias) in the BSF associated with evaporites. These descriptions instilled hope that deposits associated with subaerial exposure might be preserved, namely terra rossa, cave-fill sediments (speleothems), pedogenic carbonate, and particularly, secondary silica cements (which elsewhere have been found to contain microfossils; Horodyski and Knauth, 1994). An extensive search was conducted for these deposits.

During this study the top of the BSF was examined in several areas (see Fig. 1 and insets): (1) from Ellery Creek to about 6–7 km west of Ellery Creek, (2) from Eight Mile Gap to about 4 km east of Eight Mile Gap, (3) about 2 km on either side of Jay Creek, (4) most of the outcrops between Corroboree Rock and Ross River Station, (5) the area between the northeastern side of the Gaylad syncline and the southern part of the Mulga syncline, (6) many of the outcrops along the road west of Ringwood south of the Gaylad syncline, (7) the area immediately south of Numery Station, and (8) the area from 0 to 3 km west of the Stuart Highway about 12 km south of Henbury. As previous workers have noted, probably with some frustration, many of the strata immediately above the BSF are recessive-weathering, and thus mostly covered by younger alluvium. Where exposure is relatively good it is rarely complete. The exposures examined in detail were those that are visibly overlain by other strata, and thus preserve the identifiable top erosion surface of the BSF.

In the absence of identifiable terrestrial biota the focus shifted to expand upon previous studies and examine in detail the interval between the top of the BSF and the base of the Pertatataka

* Corresponding author. Tel.: +1 480 892 5057.
E-mail address: SJSkotnicki@aol.com (S.J. Skotnicki).

0301-9268/$ – see front matter © 2008 Elsevier B.V. All rights reserved.
doi:10.1016/j.precamres.2008.06.013

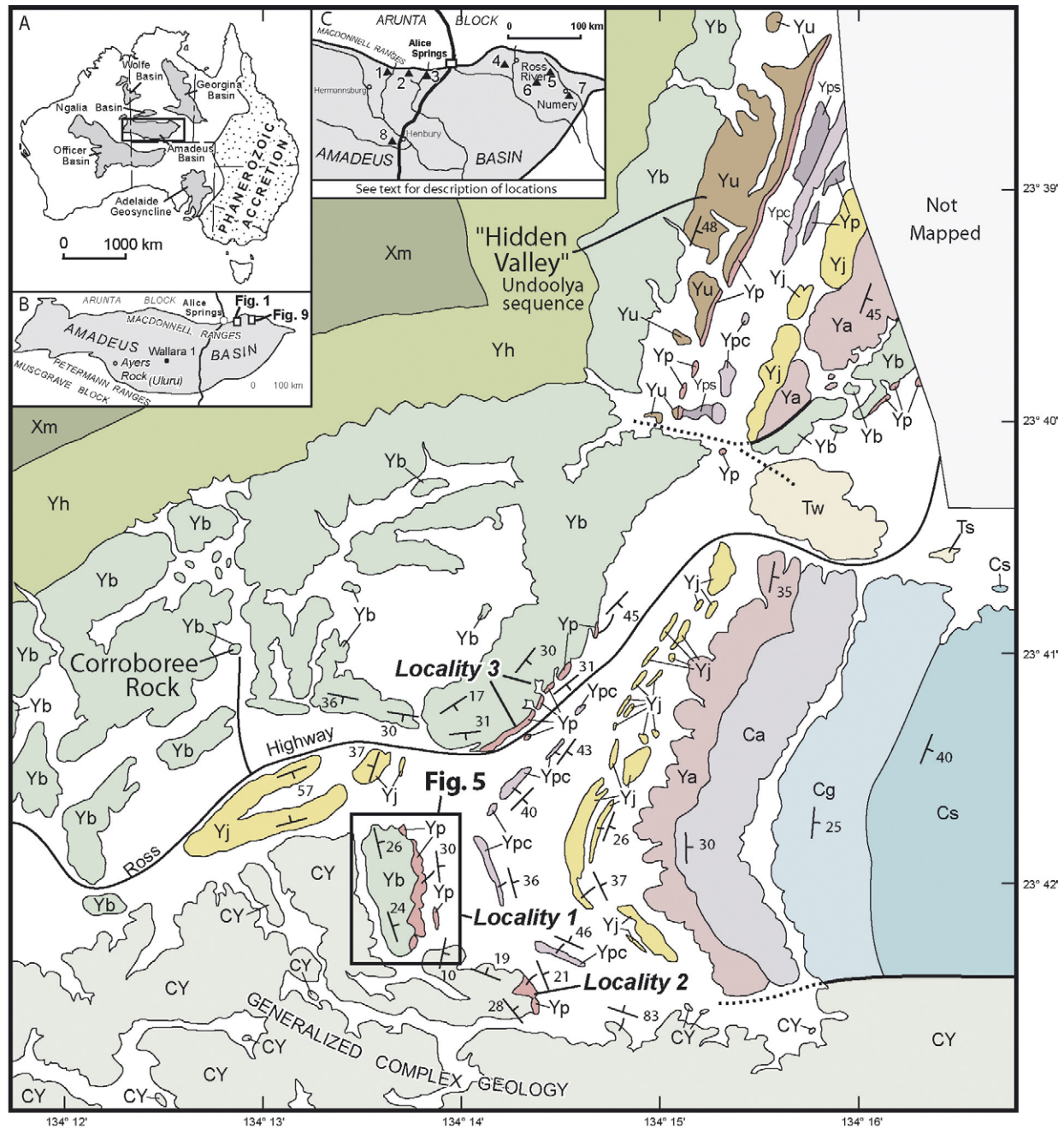

LEGEND

Quaternary
- Quaternary surficial deposits

Tertiary
- Ts — Silcrete
- Tw — Sandstone, siltstone, mudstone

0 1 km

Cambrian and Late Proterozoic
- CY — Undivided Cambrian and Late Proterozoic rocks

Cambrian
- Cs — Shannon Formation Siltstone, lm, dol
- Cg — Giles Creek Dolomite
- Ca — Arumbera Sandstone upper part

Neoproterozoic
- Ya — Arumbera Sandstone lower part
- Yj — Julie Formation Dolomite w/ minor sandstone
- Ypc — Pertatataka Formation Cyclops member, sandstone
- Yps — Pertatataka Formation Siltstone
- Yp — Pioneer Sandstone
- Yu — "Undoolya beds" Siltstone and sandstone
- Yb — Bitter Springs Formation Dolomite and siltstone
- Yh — Heavitree Quartzite

Early Proterozoic
- Xm — Metamorphic rocks Schist and gneiss

Fig. 1. Generalized geologic map of strata in "Hidden Valley" and southeast of Corroboree Rock. Bedrock-alluvium contacts mostly from aerial photographs. Geology on east side of map generalized from Shaw et al. (1983). Inset after Lindsay (1999).

Formation, particularly between Corroboree Rock and Ross River Station. Stratigraphic relationships were noted and samples were collected throughout the interval for detailed carbon ($\delta^{13}C$) and oxygen ($\delta^{18}O$) isotopic comparison of sedimentary carbonates.

2. Regional geologic setting

The Amadeus Basin is one of several large, Neoproterozoic depocenters in the heart of the Australian continent collectively referred to as the Centralian Superbasin (Walter et al., 1995; and Fig. 1, inset). The individual basins within the Centralian Superbasin all exhibit similar depositional successions of similar age that correlate closely (Preiss and Forbes, 1981; Lindsay, 1987; Shaw et al., 1991; Morton, 1997; Walter et al., 1995, 2000; Walter and Veevers, 1997; Hill and Walter, 2000). The strata in the basins are composed dominantly of sedimentary rocks, deposited in broad depressions formed on an extensive beveled erosion surface in underlying, formerly middle-crustal, middle Proterozoic granitic and metamorphic rocks. Subsequent tectonism and long-lived erosion have truncated the margins of the individual basins and have deeply eroded the successions since the Devonian, helping to create the remarkably low-relief and relatively planar profile of the Australian outback (see cross-sections in Shaw et al., 1983).

The Amadeus Basin succession contains shallow marine and non-marine sedimentary rocks that range in age from Cryogenian to Devonian (Wells et al., 1970) (Fig. 2). Sedimentation in the Amadeus Basin followed uplift and erosion that occurred during the Proterozoic Arltunga orogeny (Ding et al., 1992). The thickness of the succession is variable but locally reaches 15 km thick. The Neoproterozoic part of the succession is divided into four Supersequences separated by unconformities (Walter et al., 1995). In the oldest, Supersequence 1, initial basin formation that followed peneplanation led to the deposition of thick, widespread tidal marine sand sheets of the Heavitree Quartzite (Lindsay, 1999), followed by deposition of shallow marine carbonates, evaporites, and redbeds (marginal marine) of the BSF. Tectonic deformation during the Areyonga Movement (Wells et al., 1970; Freeman et al., 1991; Oaks, 1991) uplifted and eroded parts of Supersequence 1, resulting in a widespread unconformity represented locally by a disconformity and elsewhere by an angular unconformity at the top of the BSF. Kennedy (1993) proposed, however, that salt diapirism in the BSF rather then tectonism may be the cause of the Areyonga Movement. The unconformity is followed by sediments of Supersequence 2 which are composed of sandstone, dolomite and diamictite of the Areyonga Formation exposed in the northeastern part of the basin, and the overlying deeper-water, shale-dominated Aralka Formation (Preiss et al., 1978). The diamictites of the Areyonga Formation show evidence of glacial deposition and have been correlated with the purportedly widespread Sturtian glacial event described in the Adelaide Rift Complex.

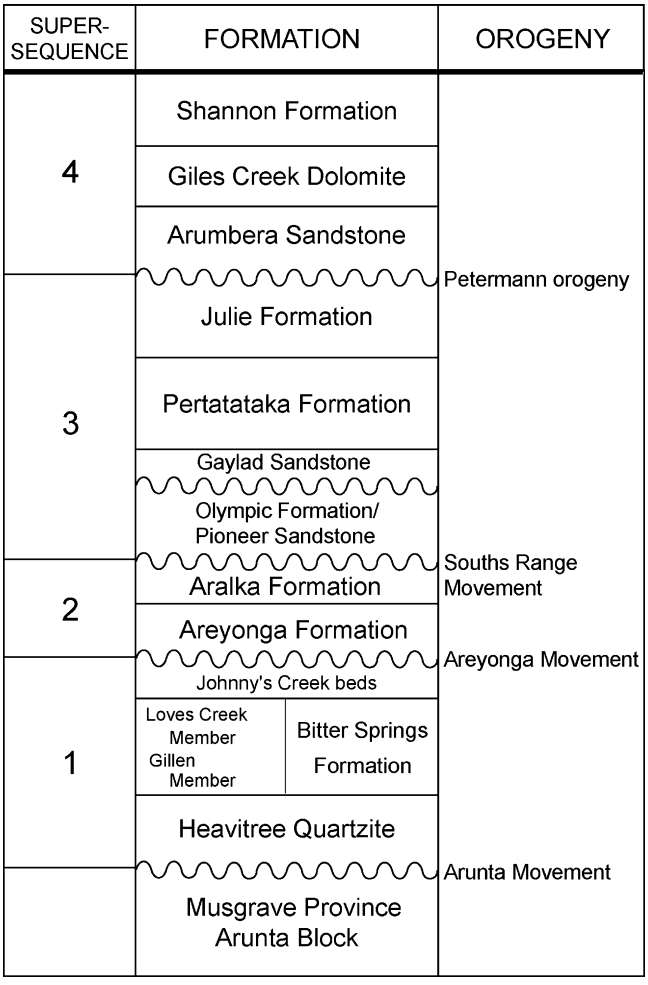

Fig. 2. Composite stratigraphic section for the Amadeus basin, central Australia.

Uplift and erosion during the Souths Range Movement (Forman, 1966; Wells et al., 1970; Lindsay, 1989; Shaw et al., 1991) was followed by deposition of Supersequence 3 composed of the nearshore Pioneer Sandstone (Lindsay, 1989) and green mudstone, sandstone, conglomerate, and diamictite of the Olympic Formation (Field, 1991). The diamictites of the Olympic Formation have been interpreted to represent a second Cryogenian glacial event (Wells et al., 1967, 1970) equivalent to the widespread 'Marinoan' glacial event (Preiss et al., 1978; Coats and Preiss, 1980; Preiss and Forbes, 1981; Knoll and Walter, 1992; Walter et al., 2000). Originally correlated with the Pioneer Sandstone, Freeman et al. (1991) recognized an angular unconformity between the top of the Olympic Formation and an overlying sandstone unit exposed near the Gaylad syncline they called the Gaylad Sandstone. The unconformity at the base of the Gaylad Sandstone merges with the unconformity at the base of the Olympic Formation to the south where they become indistinguishable (Freeman et al., 1991). The thick shale-dominated beds of the overlying Pertatataka Formation grade abruptly upward into dolomite and sandstone beds of the Julie Formation. Together, the Olympic, Pioneer, Gaylad, Pertatataka, and Julie Formations comprise Supersequence 3 and probably represent a major marine transgression (Freeman et al., 1991). The overlying deep red Arumbera Sandstone straddles the Precambrian/Cambrian boundary, and is separated from the Julie Formation by a disconformity (Kennard and Lindsay, 1991; Walter et al., 1995), representing the Petermann orogeny. The Arumbera Sandstone, Giles Creek dolomite, and Shannon Formation comprise Supersequence 4.

Neoproterozoic sedimentation in the Amadeus Basin probably began between ca. 900 and 1076 Ma. The maximum age of the inception of sedimentation is constrained by an age-date ~1076 Ma from unmetamorphosed dolerite dikes of the Stuart Dyke Swarm, which intrude gneiss of the Arunta block and are themselves truncated by the overlying Heavitree Quartzite. This recent radiometric age supersedes the older Rb–Sr age-date of 897 ± 9 Ma (Black et al., 1980), and suggests that the Stuart Dyke Swarm is coeval with the other mafic intrusions and volcanic flows across west-central Australia collectively termed the Warakurma large igneous province (Wingate et al., 2004). A U–Pb baddeleyite date of 827 ± 6 Ma for the Gairdner Dyke Swarm in the Gawler Craton and Stuart Shelf (Wingate et al., 1998) and a 824 ± 4 Ma Pb–Pb zircon date for the Gairdner Dyke Swarm in the Musgrave Complex (Glikson et al.,

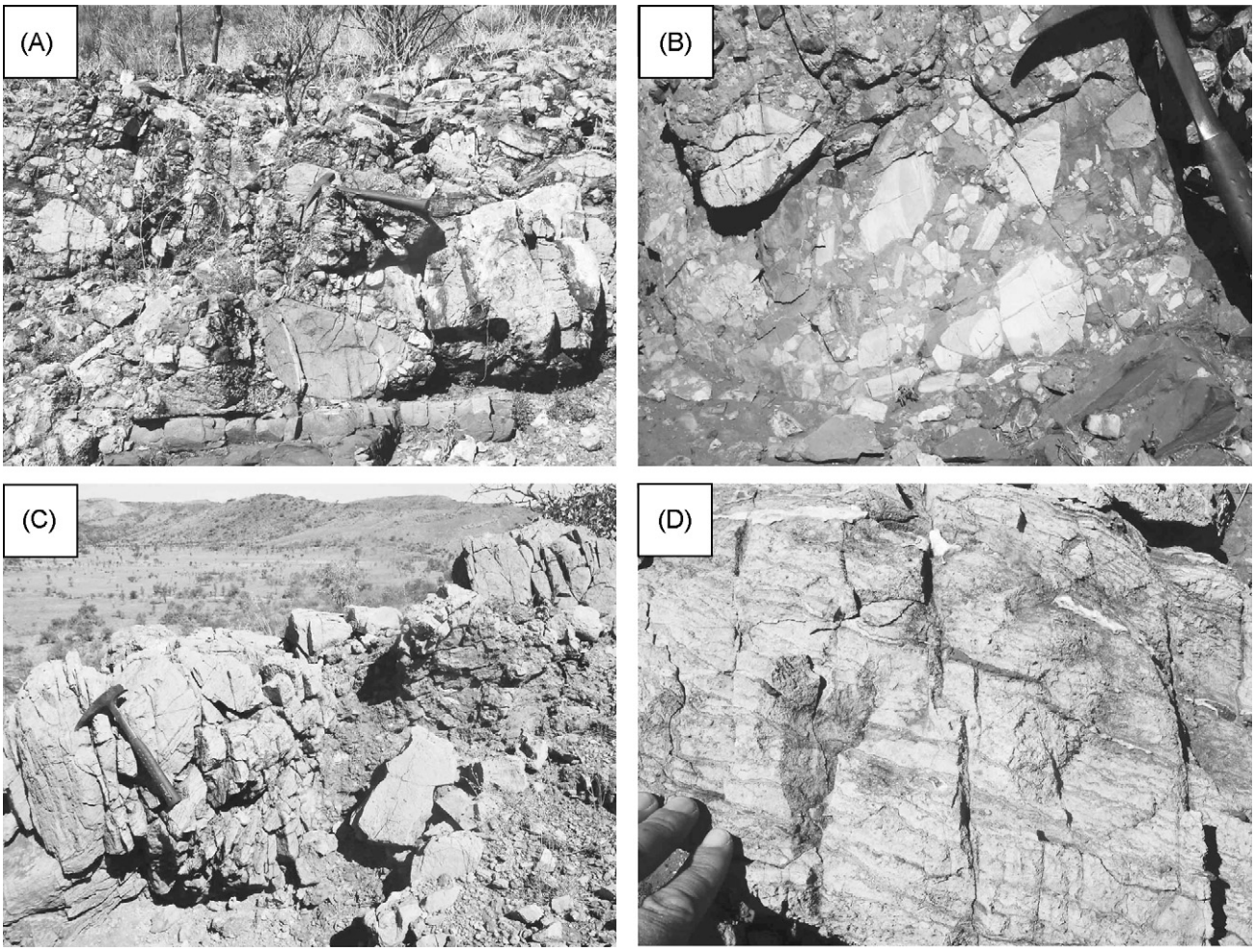

Fig. 3. Basal breccia southeast of Corroboree Rock. (A) Poorly sorted angular dolomite and chert clasts resting on erosional surface on the Bitter Springs Formation, (B) fine-grained light blue-gray dolomicrite clasts within reddish tan dolomite matrix, (C) large broken blocks of fenestrate dolomite, and (D) close-up of fenestrate dolomite block.

1996) allows a minimum estimate to be made of the initiation of Neoproterozoic sedimentation. The Gairdner dykes were probably a feeder for the Wooltana Volcanics in the Adelaide Rift Complex (Preiss, 1987), the Cadlareena Volcanics in the eastern Officer Basin (Preiss, 1987), volcanics within the Gillen Member and Unit 2 of the Loves Creek Member, BSF (Zhao et al., 1994), and the Browne Formation (Glikson et al., 1996), however, more precise dating of these formations is required before concluding they are all the same age. All these units are in contact with the underlying basal clastic sediments of the Centralian Superbasin (e.g., Heavitree and Townsend Quartzites) and Adelaide Rift Complex (Younghusband Conglomerate) that must have been deposited before ca. 830 Ma, and an estimate of ca. 840 Ma was made by Walter et al. (2000) (Fig. 2).

3. Local stratigraphic relationships

3.1. Corroboree Rock area

The area 2–3 km southeast of Corroboree Rock contains some very interesting stratigraphic relationships (Fig. 1, locality 1). Outcrops of the BSF are locally overlain by a basal carbonate breccia, in turn overlain by mature sandstone and chert-pebble conglomerate. The sandstone and conglomerate are commonly dolomitic and grade upward into poorly exposed very fine-grained dolomite. The contact between the BSF and the overlying rocks is a sharp angular unconformity with a bedding discordance of about 15–20°.

The basal breccia contains angular, very poorly sorted clasts from pebble-size to blocks more than 5 m across (Fig. 3). Three different lithologies comprise the clasts; (1) fine-grained light blue-gray dolomicrite (Fig. 3A and B), (2) light blue-gray laminoid fenestrate dolomite (Fig. 3C and D), and (3) minor chert—all surrounded by a pink-tan-colored, fine-grained dolomicrite and micrite matrix. Exposures are non-bedded and clast- to matrix-supported. The angularity of the clasts and the poor sorting indicates these deposits are not far-traveled, and are consistent with debris-flow and rock-avalanche deposits. Some of the deposits approach diamictite in texture. Kennedy (1993) observed similar deposits on the south side of the Benstead Creek structure located about 10 km northeast of Corroboree Rock. The conglomerates there contain, among others, clasts of fenestrate stromatolitic dolomite up to 2 m across. Kennedy interpreted the Benstead Creek structure as a salt-cored diapir within the BSF that was active during deposition of the BSF. He proposed that the conglomerate deposits there were the result of diapir-induced uplift and subsequent local shedding of coarse detritus. He was also aware of the breccia deposits southeast of Corroboree Rock (Walter, personal communication, in Kennedy, 1993) and proposed that they were also shed from the uplifted diapir but were subsequently transported via strike-slip movement along a south-southwest striking

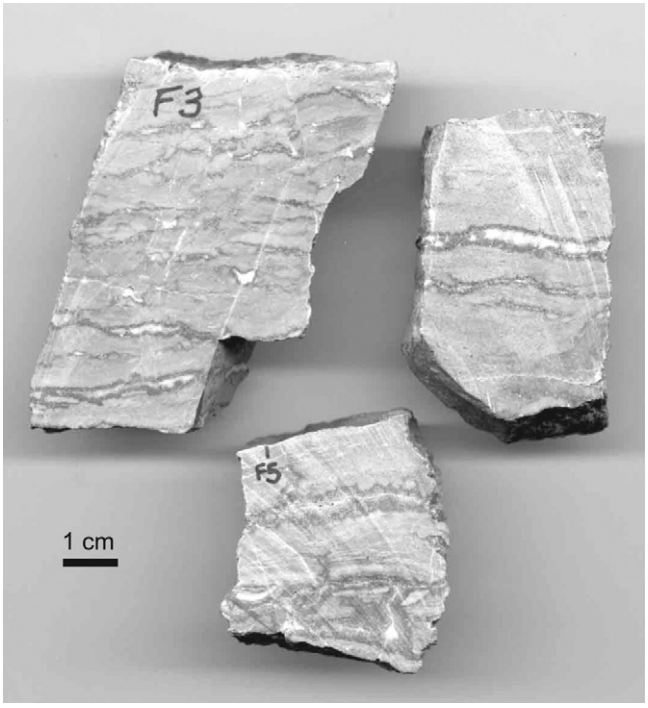

Fig. 4. Cut slabs of fenestrate dolomite clasts within basal breccia deposits southeast of Corroboree Rock. Bedding-parallel fenestrae are lined with dark, calcite spar and filled with light gray calcite spar.

fault (his F2 fault). He inferred a projection of this fault to the south, through the valley immediately to the east of the southern exposures of breccia. New mapping in the area, however (Fig. 1), does not fully support this model. Outcrops of the BSF, the Pertatataka Formation, and the Julie Formation, although mostly separated from one another by alluvium, are all consistently east-dipping and are in their correct stratigraphic positions relative to one another. It does not seem likely that the strata are offset by one or more major faults in this area.

A problem with local deposition of the breccia is the apparent lack of a source region. The fine-grained dolomicrite clasts are lithologically very similar to rocks in the underlying BSF, as are the chert clasts. However, the fenestrate clasts do not resemble any known outcrops in the BSF either nearby or in the Amadeus Basin as a whole (Fig. 4). Some stromatolite beds in the BSF show very minor fenestrate fabrics, but are nowhere nearly as well developed as the fabric within the breccia clasts. Fenestrate carbonate, particularly with laminoid fenestrae, is a common feature in some carbonates and is usually interpreted to have formed in peritidal, shallow shelf environments (Tebbutt et al., 1965) by in situ microbial mat decomposition and gas release, or by periodic sea-level fall accompanied by selective dissolution in the vadose zone. Some lacustrine travertine deposits also exhibit fenestral fabics, and the term "tufa" has been commonly applied to both marine and lacustrine fenestral carbonate (Grotzinger, 1986; Demicco and Hardie, 1994).

It is possible that the fenestrate fabric in the breccia clasts at locality 1 developed much later, after breccia deposition, by later alteration, but the prevalence of fenestrae parallel to bedding planes within individual clasts, now rotated with respect to one another, and the similarity of this fabric to widely studied fenestrate fabrics elsewhere argues against later alteration and suggests it is an early diagenetic fabric. To attempt to determine if the fenestrate clasts originated from the BSF the $\delta^{18}O$ and $\delta^{13}C$ compositions of these clasts were analyzed and compared to the isotopic values of the non-fenestrate dolomicrite clasts, the dolomicrite matrix, and the underlying BSF. The coarse-grained dolospar filling the fenestrae was also analyzed. Results of the analyses are shown in Fig. 5.

Interbedded sandstone and conglomerate between 5 and 10 m thick overlying the breccia (Fig. 6A) contain a nearly bimodal assemblage of well-rounded light gray banded chert pebbles and larger, 5–30 cm-wide, rounded to angular dolomite clasts, all in a rather mature, well-sorted, thinly bedded quartz sand matrix (Fig. 6C–E). The well-rounded chert pebbles are probably far-traveled and may represent an older, more mature population, whereas the more poorly sorted and angular dolomite clasts are more likely locally derived. The sandstone is commonly dolomitic and grades both laterally and vertically into layers dominated by dolomite (Fig. 6E). In areas dominated by dolomite, some chert pebbles appear to 'float' within the carbonate (Fig. 6B). The dolomite itself is commonly massive to faintly laminated, is very light tan to pink on fresh surfaces, and is very fine-grained characteristics similar to the descriptions of 'cap dolomites' above Neoproterozoic glacial units. The $\delta^{18}O$ and $\delta^{13}C$ compositions of this dolomite were analyzed to compare to values from dolomites farther north interpreted as cap dolomites and to cap dolomites elsewhere in Australia.

In the limited exposures visible, dolomitic sandstone and conglomerate grades upward into beds several tens of centimeters thick of nearly pure dolomite. This uppermost dolomite is capped by a thin, 10 cm-thick layer of silicified stromatolites (Figs. 4, and 6F and G) composed of Elleria minuta (Walter, 1972), possibly synonymous with Anabaria = Kotuikania juvensis (Williams et al., 2007).

In the southernmost exposures (locality 2) the BSF is overlain discordantly by a thick succession (>15 m) of thin- to medium-bedded brown sandstone. The basal 2 m of the succession is a conglomerate containing sub-angular to rounded dolomite pebbles and cobbles. Bedded calcarenite 2–5 m thick overlies the conglomerate and grades into overlying sandstone containing grains of quartz and recognizable chert granules. The upper part of the sandstone succession contains abundant lenses of chert-dolomite pebbly conglomerate up to several tens of centimeters thick. The very top of the succession, as at locality 1, grades abruptly upward into interbedded chert-pebble conglomerate and dolomitic sandstone, which grades into a pure dolomite bed several tens of centimeters thick. This dolomite is interpreted to be equivalent to the dolomite in the upper portions of locality 1. Two samples of dolomite were analyzed for their $\delta^{18}O$ and $\delta^{13}C$ ratios (samples CR1 and CR2) and results of which are shown in Fig. 5.

Interestingly, rare, small, rounded pebbles of red chert found within the pebble conglomerate at locality 1 are all composed of coarse-grained quartz, quite unlike the majority of chert clasts in the deposits which are composed mostly of granular microcrystalline (Gm) quartz. These clasts also exhibit disrupted microfabrics composed of hematite. Field (1991, p. 131) also apparently noted the existence of these red pebbles within the sandy lithofacies of the Olympic Formation, but the source for them is unknown. Similarly, rare red pebbles composed of coarse-grained quartz and containing disrupted hematite fabrics were also observed in basal sandstone and conglomerate overlying the middle Proterozoic Mescal Limestone in Arizona. Whether or not the clasts in each locality have a common source is unknown.

3.2. Northeast of Corroboree Rock along the Ross Highway

About 2 km east of Corroboree Rock the Ross Highway parallels strike-ridges of the tilted top of the BSF. Here, a bed of dolomite ~2 m thick rests directly on top of the BSF. Rather then a discrete bed, however, the dolomite is composed of sub-angular to sub-rounded dolomite 'clasts' up to about 30 cm across surrounded by a dolomite matrix. The dolomite in the matrix appears identical to the

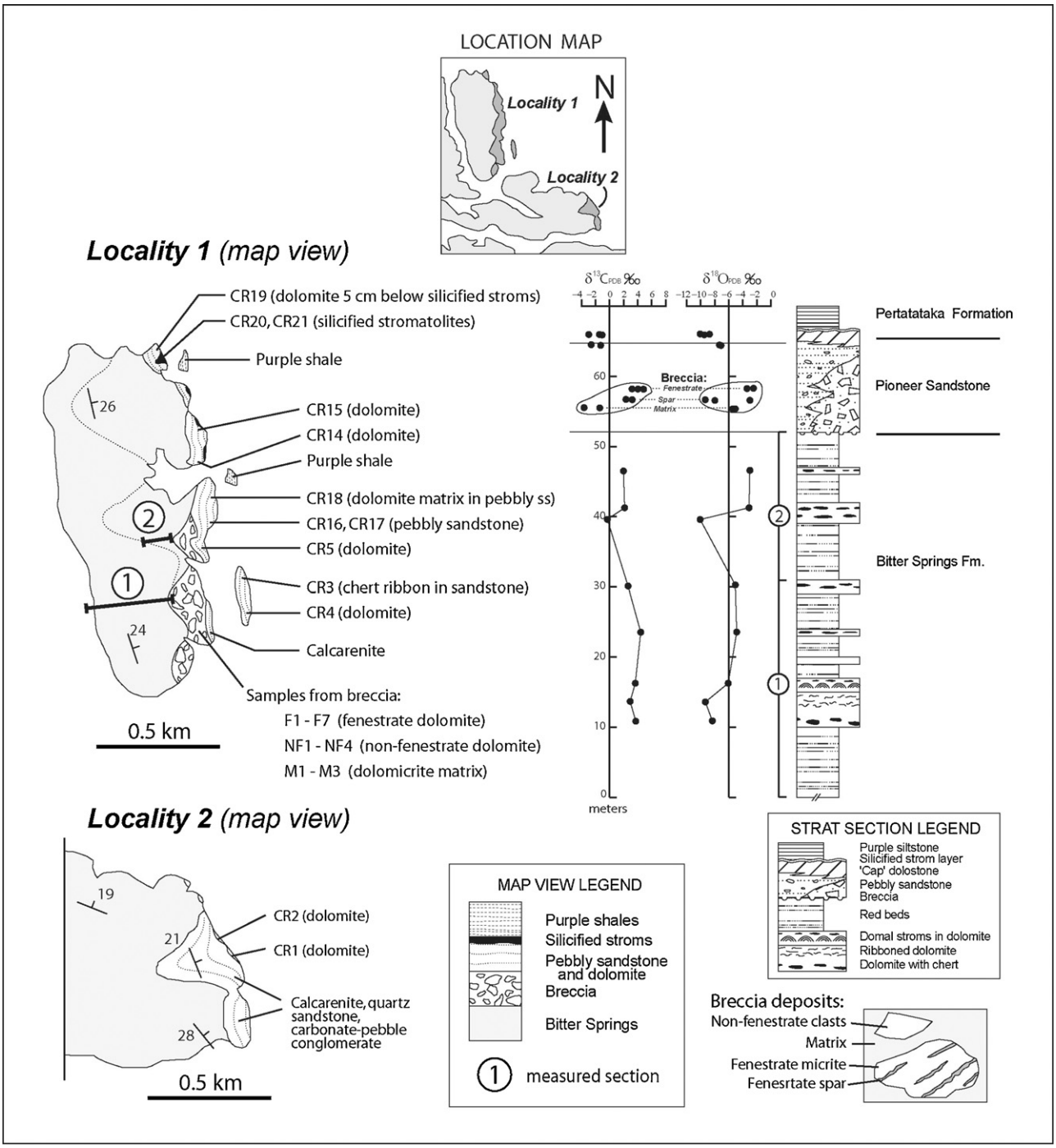

Fig. 5. Maps and stratigraphic section of localities 1 and 2, southeast of Corroboree Rock, showing geology and stable isotope relationships between the Bitter Springs Formation, the various clast types within the basal breccia (of the Pioneer Sandstone), and the 'cap carbonate' at the base of the Pertatataka Formation.

dolomite in the clasts. Both are tan-colored to light pink on fresh surfaces, very fine-grained, and show abundant manganese dendrites on fracture surfaces. The brecciated nature of the bed is not obvious everywhere because of the similarity between the clasts and the matrix. Locally, visible internal stratification is defined by finely granular beds and/or faint laminations. The lower parts of this bed locally contain minor carbonate breccia and more abundant chert-pebble conglomeratic quartz sandstones similar to the beds farther south.

As with the exposures to the south the top surface of the dolomite bed is capped by a thin layer of silicified stromatolites (Elleria minuta; Walter, 1972) typically between 10 and 20 cm thick. In several outcrops the silicified stromatolite layer wraps up and over mounds of breccia a few meters across and up to 1 m high (Fig. 7). These mounds apparently represent original relief on the upper surface of the dolomite bed. Kennedy (1993) observed this stromatolite bed wrapping over similar mounds and interpreted the mounds as stromatolitic bioherms. At least in the exposures described here along the road, however, the internal composition of these mounds is entirely dolomite breccia, and only the very top surface is covered by stromatolites. Hence, these mounds are not bioherms per se because they

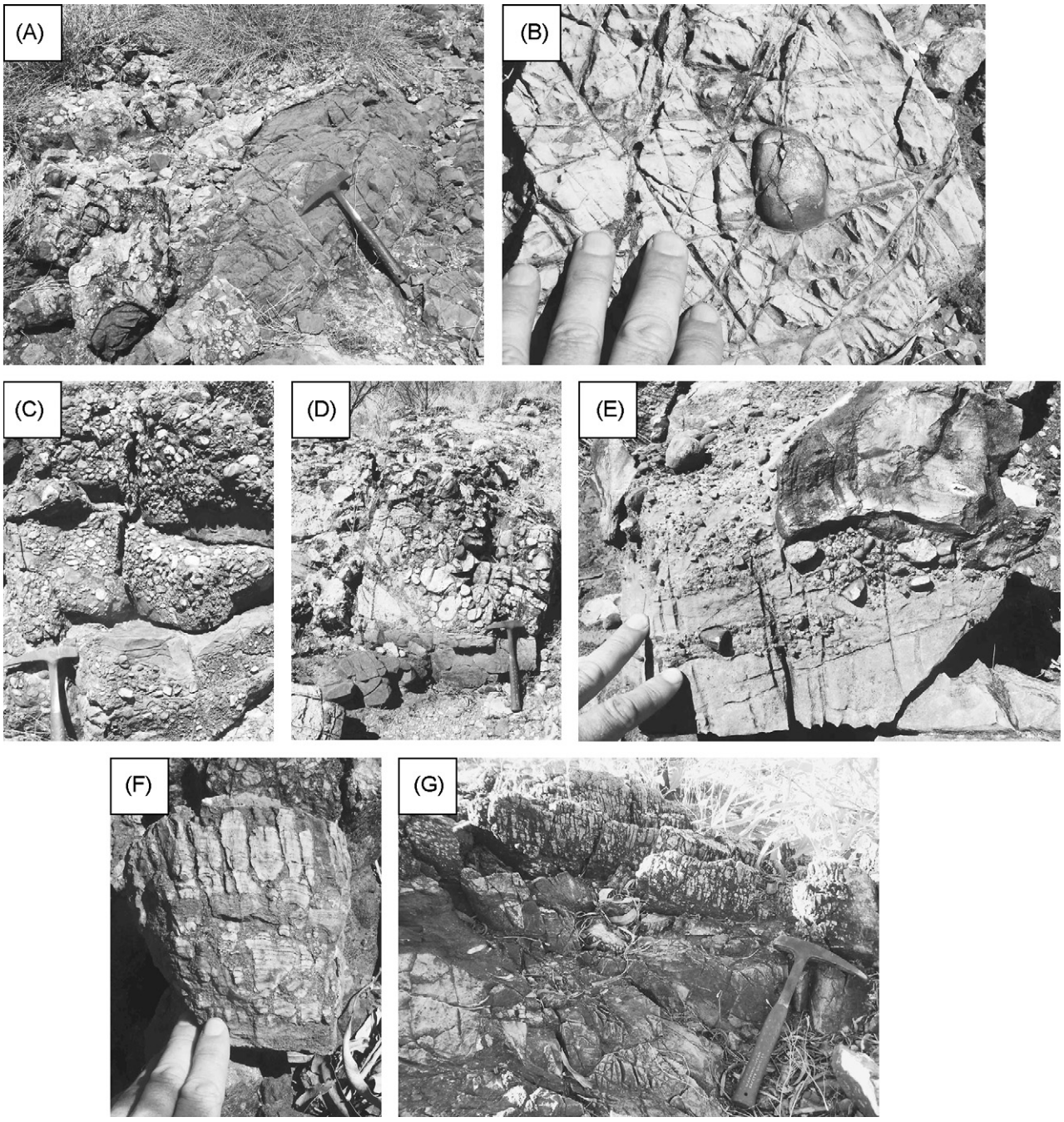

Fig. 6. Outcrops of the Pioneer Sandstone southeast of Corroboree Rock. (A) Disconformable contact between Bitter Springs Formation (at hammer) and Pioneer Sandstone above. (B) Close-up of rounded chert pebble 'floating' in fine-grained dolomicrite. (C) Chert-pebble and dolomicrite-pebble clasts within fine-grained quartz sand and dolomicrite matrix. (D) Poorly sorted clasts of dolomicrite and minor chert in light gray sandy dolomicrite matrix. (E) Close-up of exposure showing large angular dolomicrite clasts in a bedded horizon containing mostly chert pebbles within sandy fine-grained dolomicrite. (F) Hand sample showing columnar structure of Elleria minuta. (G) Typical subdued outcrop of Elleria minuta (above hammer) grading abruptly into fine-grained dolomicrite below.

were not created by the buildup of organisms but, instead, were allochthonous.

3.3. Hidden Valley

A few kilometer north of the exposures along the road, a strike-valley, here informally called Hidden Valley (Fig. 1), contains a thick enigmatic succession of brown sandstone and siltstone which Kennedy (1993) called the Undoolya sequence (Fig. 8). Over 700 m thick, this succession unconformably overlies the BSF and

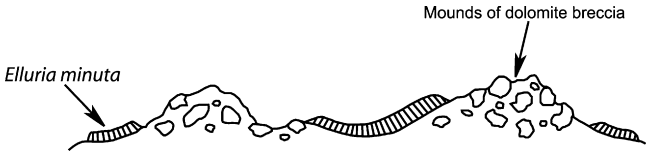

Fig. 7. Diagram illustrating the observed relationships between the Elleria minuta and the underlying cap dolomite breccia, about 2 km east of Corroboree Rock along the Ross Highway. Elleria minuta bed appears to wrap up and over mounds of breccia.

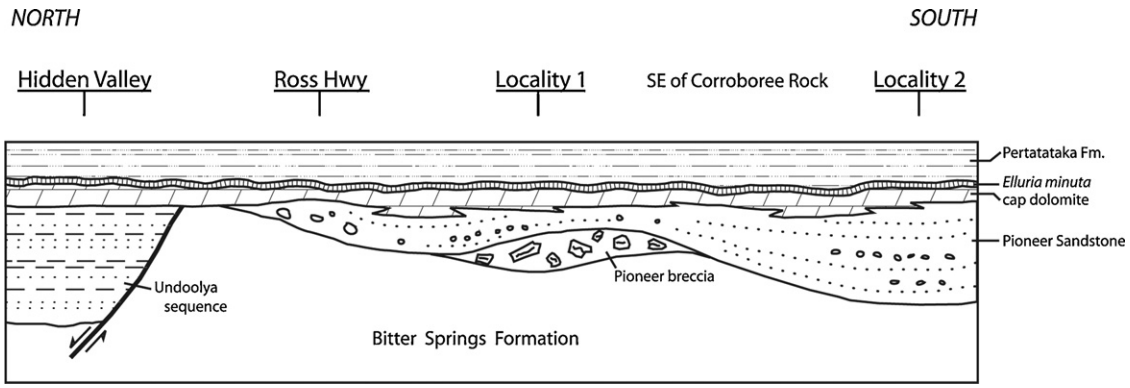

Fig. 8. Diagrammatic illustration showing the relationships between units deposited above the Bitter Springs Formation erosion surface between Hidden Valley and Corroboree Rock. The Pioneer Sandstone and breccia rest on an angular unconformity atop the Bitter Springs Formation. The Pioneer Sandstone is dolomitic upward and grades abruptly into the overlying cap dolomite. Movement on the fault at the south end of Hidden Valley is shown as it appeared at the end of deposition of the Undoolya sequence (Kennedy, 1993).

is exposed nowhere else in the region (Kennedy, 1993). Kennedy noted the facies and thickness changes towards what he interpreted as the probable salt-mobilized diapiric Benstead Creek structure at the northern end of the valley and concluded that the Undoolya sequence was deposited in a local sag created by salt removal adjacent to the diapir. The sedimentary succession thins gradually to the south where it is abruptly truncated by an east-southeast-trending fault that here is interpreted to connect with Kennedy's southwest-trending F2 fault. A branch of this fault likely projects southeastward under Tertiary sandstone and siltstone (map unit Tw in Fig. 1) but the continuity of stratigraphy farther south of this fault suggests that it is unlikely that the F2 fault continues to the south as Kennedy (1993) suggested. The absence of the Undoolya sequence south of this fault indicates that the fault was active at least as early as the end of deposition of the BSF.

The upper part of the Undoolya sequence to the south consists of thin-bedded dolomitic sandstone and siltstone and is sharply overlain by a 1–2 m-thick dolomite bed that forms a prominent, east-dipping, resistant ridge. The dolomite bed weathers dark brown, but is light tan to pink on fresh surfaces, is very fine-grained, exhibits manganese dendrites on joint surfaces, and resembles the dolomite bed described farther south. The dolomite bed in Hidden Valley is locally sandy and laminated, but, like exposures along the road to the south, in places is dolomite breccia consisting of sub-rounded to sub-angular cobble-size dolomite clasts surrounded by a dolomitic matrix of nearly identical composition.

In both laminar and brecciated areas the dolomite bed contains deep red, irregularly shaped chert nodules between 2 and 40 cm across. Some cherts are lenticular with their long axes parallel to the bedding plane of the dolomite. In outcrop, most of the cherts show no preferentially aligned internal structure and contain chaotic microfabrics. With a hand-lens faint, wispy laminations in some cherts are seen to be composed of crudely alternating red and light gray laminae. Thin-sections reveal that the red color of the cherts is due to abundant fine-grained hematite. Red globuse forms up to 1–2 mm across are commonly cored by spherules of fibrous quartz. Light gray areas are composed of minor granular microcrystalline quartz, but more commonly coarser-grained microcrystalline quartz that exhibits the irregularly shaped grain boundaries of Gm but possesses individual crystals greater than 30 μm across. These lighter gray areas also contain interlocking irregularly shaped areas of fibrous quartz. Thin veins of megaquartz cut all fabrics. Silica rhombic pseudomorphs suggest the Gm replaced the original carbonate.

This dolomite bed is also capped by a layer of silicified columnar stromatolites ~10 cm thick, immediately overlain by fissile purple shales of the Pertatataka Formation, indicating that the dolomite bed atop the Undoolya sequence is equivalent to the dolomite bed farther south. The thicknesses of the overlying Pertatataka and Julie Formations are consistent both in Hidden Valley and to the south, indicating that movement along the bounding fault on the south side of Hidden Valley ceased for a time prior to deposition of the dolomite bed, before renewing again sometime after deposition of the Julie Formation and possibly the Arumbera Sandstone.

3.4. Ross River

The Ross River locality, 1–2 km north-northeast of Ross River Station (Fig. 9), contains one of the best exposed sections of the BSF in the Amadeus Basin (Fig. 10A). The lower Gillen Member is locally folded and overturned, and two narrowly spaced northwest-striking faults cut through both members, but overall both members of the BSF form an almost continuous succession over a distance of ~1 km. Most of the succession dips between 30° and 70° to the south. The uppermost 40 m of the BSF was measured and sampled as were the overlying formations.

At the measured section the BSF is overlain by 5 m of thin- to medium-bedded brown quartz sandstone and pebbly conglomerate containing sub-angular to well-rounded pebbles of chert and carbonate. This unit is overlain by a conglomerate/breccia that contains mostly sub-angular to sub-rounded dolomite clasts, and minor chert (Fig. 10B). This is also the location of the famous black chert microfossil locality originally described by Schopf (1968). Many of the dolomite clasts have a laminoid fenestral fabric, and in this respect this unit is similar to the breccia unit described east of Corroboree Rock. Although the source of the fenestrate dolomite is uncertain, conglomerates containing clasts exhibiting this fabric are characteristic of the Pioneer Sandstone, and we interpret the underlying brown sandstone and conglomerate and the upper conglomerate/breccia to belong to the Pioneer Sandstone. About 1 km to the east of the measured section the formation thickens to about 10 m where it forms a dip-slope on the south side of the ridge.

Overlying the Pioneer Sandstone is a small exposure of dolomite about 5 m thick (Fig. 10C) in turn overlain by Quaternary sediments. The dolomite is massive to locally weakly laminated, weathers light brown, and is chert-rich. On fresh surfaces the dolomite is light tan and is very fine-grained dolomicrite and dolospar. The cherts occur as angular nodules from less than 1 cm to over 10 cm across. They display a wide range of colors, from light tan near the base, deep red near the middle, and light gray to black near the top of the exposure (Fig. 10D). The cherts mostly occur in discrete beds up to about 10 cm thick. Curiously, however, many of the

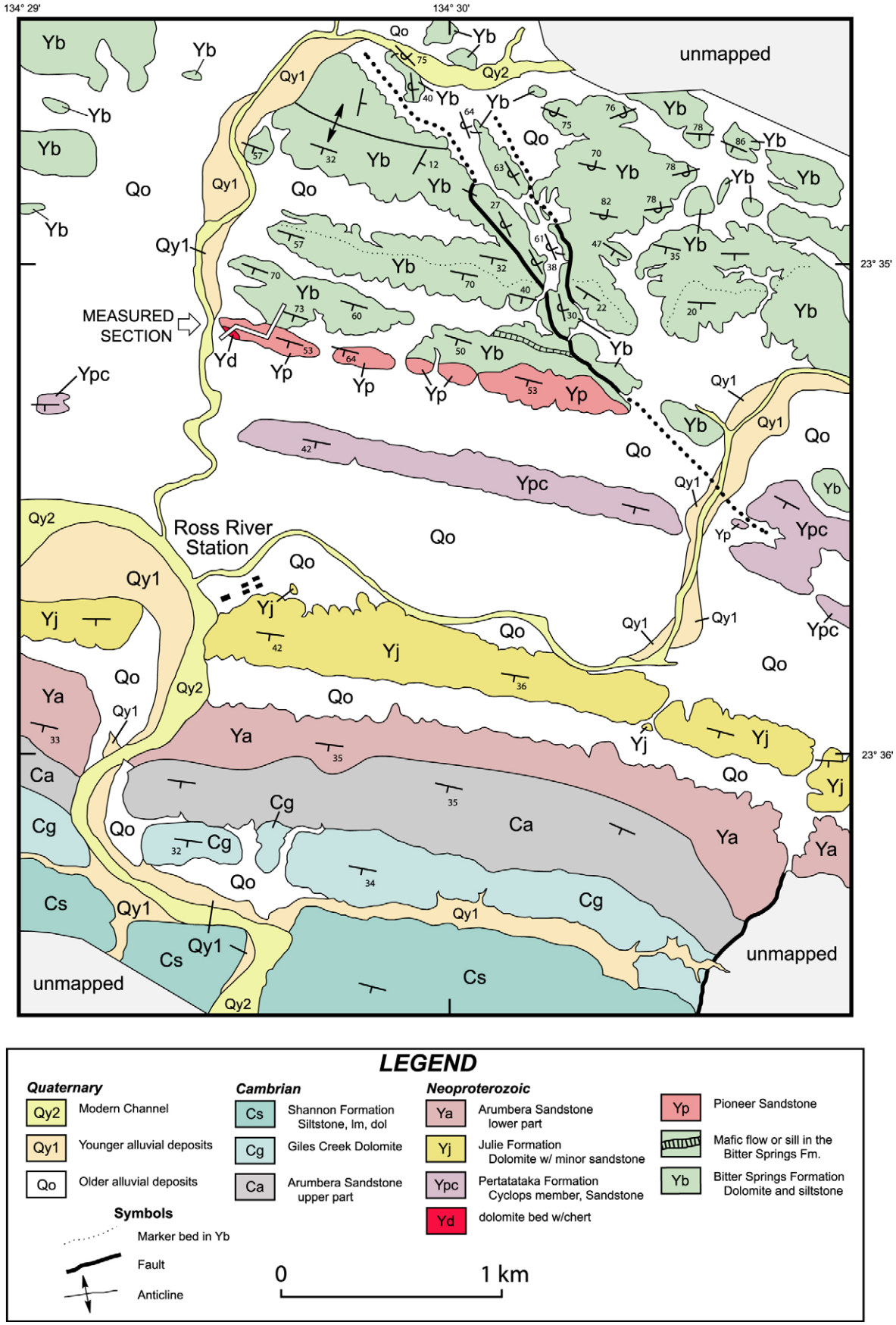

Fig. 9. Generalized geologic map of the Ross River Station area, showing location of sampled section. Bedrock-alluvium contacts mostly from aerial photographs.

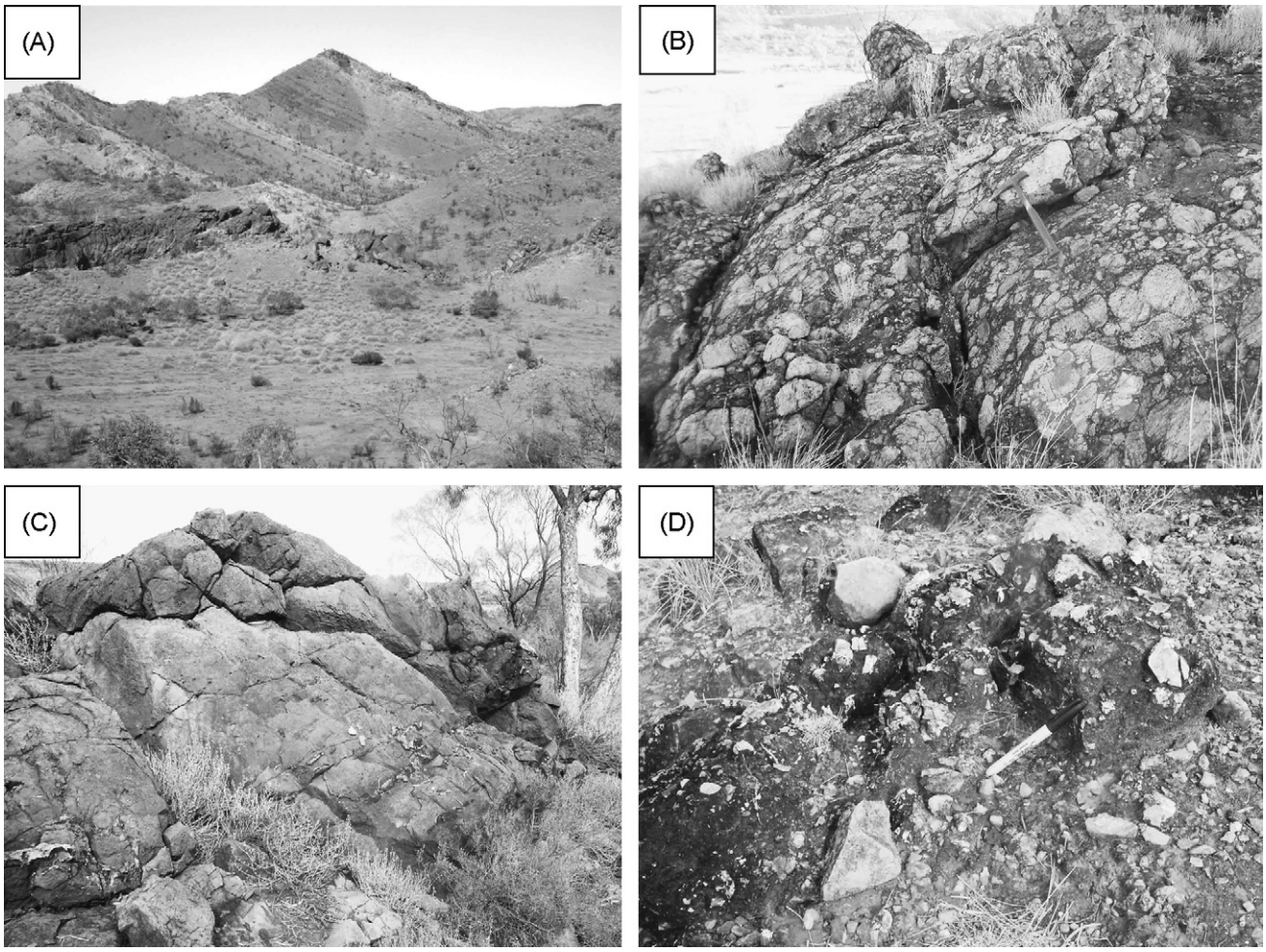

Fig. 10. Outcrops of the Bitter Springs Formation and overlying units north of Ross River Station. (A) South-tilted section of the Bitter Springs Formation, looking east-southeast. (B) Outcrop vies of the Pioneer Sandstone showing sub-rounded cobbles of fenestrate dolomite and dolomicrite within a sandy dolomitic matrix. (C) Outcrop view of 'cap carbonate' (labeled Yd in Fig. 8) overlying Pioneer Sandstone, looking west. Light gray chert stringers visible in lover part of outcrop. (D) Close-up of upper part of outcrop showing brecciated, chaotic nature of chert within the dolomite.

cherts appear partly shattered and brecciated (Figs. 10D, and 11). No obvious brecciation is visible in the surrounding dolomite, however the near absence of recognizable bedding within the dolomite may be obscuring brecciation. In thin-sections, all of the cherts are composed chiefly of two textures: granular microcrystalline quartz and fibrous quartz. Darker-colored areas within cherts are composed mostly of Gm, whereas lighter colored areas are composed of interlocking botryoidal fans of fibrous quartz. The botryoidal forms locally line former cavities that were subsequently filled with megaquartz. Some fibrous quartz occurs in irregularly shaped patches throughout areas composed of Gm. In some sections euhedral dolomite grew atop the cavity-lining botryoids before being overgrown by megaquartz. Abundant euhedral dolomite rhombs 'floating' within the Gm suggests these cherts formed by silica replacement of original carbonate.

3.5. Gaylad/Mulga synclines

The area between the Gaylad and Mulga synclines is covered by broad, low-lying hills composed mostly of clean, medium- to coarse-grained feldspathic sandstone. Although mapped by previous workers as Pioneer Sandstone and correlated with the Olympic Formation (Shaw et al., 1983; Preiss et al., 1978), Freeman et al. (1991) observed a regional angular unconformity between this unit and the Olympic Formation near Dead Horse Water Hole on the Hale River and gave the sandstone the new name, Gaylad Sandstone. However, the angular unconformity merges southward with the unconformity at the base of the Olympic Formation (Freeman et al., 1991), and the two formations become indistinguishable. Field (1991) also suggested that the Pioneer Sandstone at Ellery Creek and the Gaylad Sandstone may be equivalent. In any case, the shallowly south-southeast-dipping sandstone exposed in the dissected hills between the Gaylad and Mulga synclines directly overlies the BSF and locally the contact is well-exposed.

Good exposures of the contact are found in the southeastern-most part of the hills where erosion has created several small fensters into the underlying BSF. Here, the BSF is overlain in a sharp contact by a 0–2 m-thick conglomerate containing sub-angular to well-rounded pebbles and cobbles of dolomite apparently derived from the underlying BSF. The dolomite clasts are surrounded by a quartz sand matrix and cemented by silica. The quartzose matrix is identical to immediately overlying beds of the Gaylad Sandstone.

On the northwest side of the hills, deep dissection has revealed the same 0–2 m-thick dolomite-clast conglomerate overlain by feldspathic sandstone (Fig. 12). The conglomerate grades laterally into pebbly dolomitic quartz sandstone that weathers dark and forms a distinctive dark band just above the contact with the BSF (Fig. 12A). As Freeman et al. (1991) described previously, the uppermost 1–2 m of the BSF here contains vertical and horizontal sandstone lenses that appear to have filled enlarged dissolution

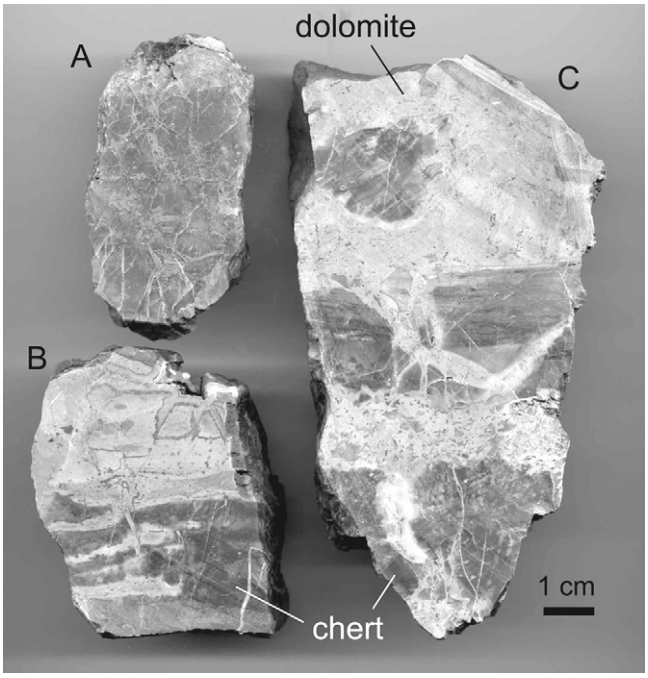

Fig. 11. Cut slabs of dolomite and chert within cap carbonate north of Ross River Station. Section A is a dark red chert clast from the middle of the unit. Sections B and C are from near the exposed top of the unit and contain black cherts.

joints in the very top of the formation (Fig. 12B and C). In at least one area (Lat-Long 23° 40.20′S, 134°50.43′E; UTM 7379000N, 53491000E) these dissolution joints are filled with silica and form a box-work network of silica 'veins' that stand out as resistant ribs on weathered surfaces (Fig. 12D). Box-work silica has previously been interpreted as having characteristically formed in uplifted and subaerially exposed carbonates (Hill and Forti, 1997). Although rare, vertical silica-filled veins (grikes) are exposed in a few other places along the top of the BSF in this local area.

In thin-section the silica from the box-work and from the silica grikes are all composed of similar types of chert: normal and zebraic chalcedony forms large, interconnected botryoids up to ~0.75 cm wide and is overgrown by elongate, fan-shaped crystals of megaquartz up to 1 cm long. The chalcedony appears to have lined the walls of former cavities in the top of the BSF (Fig. 13). The elongate quartz crystals are in sharp contact with the underlying chalcedony, are commonly in crystallographic continuity with the chalcedony, and form euhedral terminations toward the centre of the former cavity. The remaining space was subsequently filled with irregularly shaped crystals of megaquartz. This succession is typical of those found in silica-filled cavities world-wide.

The wall rock onto which the silica nucleated and grew is composed both of BSF black chert and dolomite. In thin-sections the black cherts have been modified and apparently dissolved such that the formerly exposed surfaces are locally bulbous and highly irregular. In some black cherts beautifully preserved nests of filamentous microfossils are truncated at the edges of bulbous projections by overlying chalcedony botryoids. The meteoric water that dissolved these black cherts must have been undersaturated in silica compared to the water that precipitated the box-work silica that must have been supersaturated in silica.

Almost all of these silica veins fill former cavities in the top of the BSF. One such feature was found cutting the dolomite-clast conglomerate immediately overlying the top of the BSF (Fig. 12E). It contains the same chert fabrics as those immediately below. Rare, thin white quartz veins up to ~8 mm wide were locally found in pieces of float from the overlying sandstone, but in thin-section they are composed wholly of megaquartz and do not contain the same fabrics as the underlying chert veins. The fact that most of the veins are found only in the top 1–2 m of the BSF, where they form a box-work and are associated with sandstone-filled cavities, suggests that the silica precipitated after exposure of the BSF and before deposition of the sandstone. However, the presence of the lone silica vein in the conglomerate is puzzling, and shows that at least some of the silica precipitated after deposition of the conglomerate, apparently in fractures. The apparent absence of similar chert veins in the overlying sandstone suggests that the silica is older than the sandstone.

4. Methods

Carbonate samples were collected that were representative of the interval, and were free of as much visible siliciclastic material as possible. Thin-sections were made of some of the samples, and effort was made to select regions within each sample that exhibited a micrite or microspar crystal size, except for the samples specifically collected because they were more coarsely crystalline. A very small carbide-tipped steel drill bit was used to select and powder each sample. Site selection and drilling was done using a binocular microscope. The $\delta^{18}O$ values of dolomite were corrected for mineralogy. Twenty milligram powdered samples were dissolved in phosphoric acid in evacuated glass vessels and analyzed in Paul Knauth's mass spectrometer at Arizona State University. The isotope ratios were measured relative to an internal gas reference standardized with respect to the international standard NBS-19 and reported on the V-PDB scale. These values are reported in Table 1.

5. Discussion

5.1. Brecciation of cap dolomite

As mentioned above brecciation in the cap carbonate was seen in outcrops along the Ross Highway, in Hidden Valley, and at Ross River. At Ross River the carbonate is mostly massive and brecciation is revealed by broken and rotated angular clasts of chert. Southeast of Corroboree Rock the carbonate is mostly massive to weakly laminated dolomicrite and contains abundant siliciclastic detrital grains. The underlying Pioneer Sandstone (as mapped at locality 1, Fig. 1) thickens southward in the same area where brecciation in the overlying pink carbonate is not apparent. In fact, as mentioned above, there is no discrete cap carbonate southeast of Corroboree Rock (at least not exposed). Instead, the Pioneer Sandstone becomes more dolomitic upsection.

Because the pink/cap carbonate is at most 2–3 m thick it is highly unlikely the brecciated areas represent a basal karstic collapse breccia formed during a subaerial exposure event. There are no obvious solution cavities nor secondary cements indicative of subaerial exposure. Because of the lateral pervasiveness of this unit without significant thickness changes, and its apparent conformable relationship to the underlying Pertatataka Formation, its origin as a debris flow or avalanche deposit from a local topographic high is also unlikely. The unique petrography of this carbonate and the lack of a source region also argue against a debris flow origin.

Instead, calm-water deposition of fine-grained dolomicrite may have been followed by turbulent flow strong enough to brecciate the deposit. The presence of discrete dolomicrite clasts, many with sub-rounded sides, indicates the carbonate was already at least partly lithified before brecciation. Emergence and fluvial reworking would have produced clasts of dolomite, however the cements

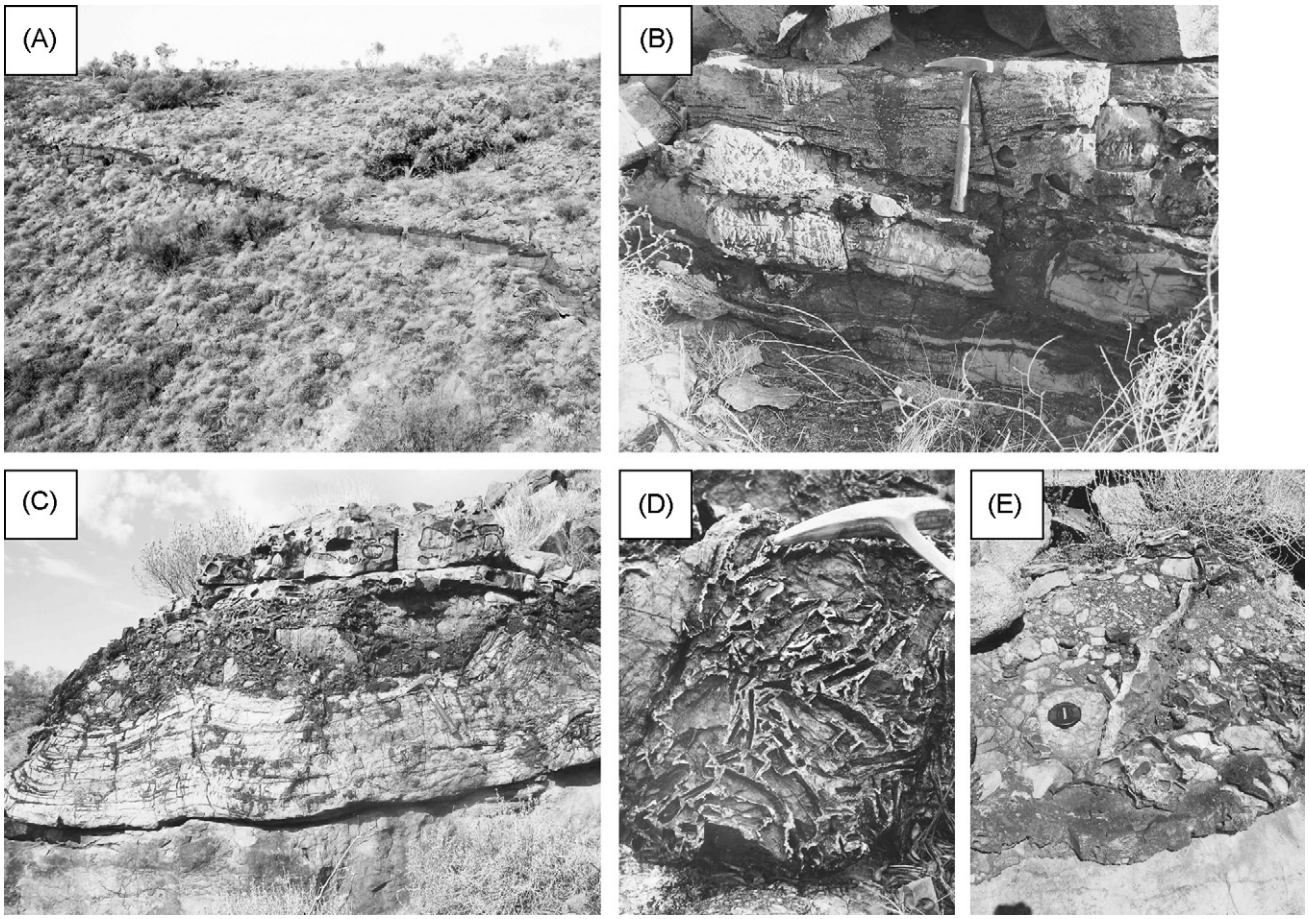

Fig. 12. Exposures of karsted Bitter Springs Formation and overlying units on the north side of the Gaylad Syncline. (A) Pebbly dolomitic quartz sandstone weathers dark and forms a distinctive dark band just above the contact with the Bitter Springs Formation, separating it from the Gaylad Sandstone above. (B) Darker sandstone fills enlarged dissolution joints in the upper 2 m of the Bitter Springs Formation. (C) Outcrop showing Gaylad Sandstone disconformably overlying and filling vertical and horizontal dissolution joints within the underlying Bitter Springs Formation. (D) Box-work silica veins protruding from less-resistant dolomite of the Bitter Springs Formation immediately below the contact with the overlying Gaylad Sandstone. (E) Silica-filled grike in dolomitic conglomerate immediately overlying the Bitter Springs Formation.

between clasts produced in the subaerial environment should be distinct from the dolomite in the clasts, but they are petrographically identical. Also, the fine-grained shales of the immediately overlying Pertatataka Formation indicate submergence in a deeper-water environment.

5.2. Interpretation of Elleria minuta

Elleria minuta (apparently synonymous with Anabaria = Kotuikania juvensis, Williams et al., 2007) is a stromatolite that grew in erosional hollows on the upper surface of supposed 'Marinoan' cap dolomite in the Amadeus Basin (Walter et al., 1979). The apparent ubiquity of the silicified stromatolite layer makes it a useful datum. It is widespread across the northeastern Amadeus Basin, and is always stratigraphically above the BSF and below the Pertatataka Formation. $\delta^{13}C$ data in this paper and limited stromatolite biostratigraphy (Grey et al., 2005) combine to support a correlation with the Marinoan glacial succession elsewhere in Australia. Elleria minuta is characteristically columnar and silicified by bluish gray granular microcrystalline quartz (chert). The interspaces between the silicified columns are commonly composed of light tan to pinkish tan dolomicrite (Fig. 4). In several exposures the interspaces contain abundant sub-angular coarse-grained quartz sand. The presence of these quartz-sand-filled interspaces in areas directly overlying dolomite of the BSF suggests parts of the Pioneer Sandstone may have been reworked during deposition of the stromatolite bed. This may indicate relatively shallow-water tidal or wave-influenced environments.

5.3. Stable isotopes

5.3.1. Corroboree Rock data

5.3.1.1. Bitter Springs Formation $\delta^{13}C$ and $\delta^{18}O$ stratigraphy. The $\delta^{13}C$ stratigraphy of the BSF at Corroboree Rock, as shown in Fig. 5, closely resembles that in the uppermost parts of Unit 3 of the Loves Creek Member (Hill et al., 2000), as well as the overlying Johnnys Creek beds (formerly called the Finke beds) in drill hole Wallara 1 (Hill et al., 2000), where the values are mostly between +2 and +4‰. $\delta^{13}C$ values of +4 to +6/+7‰ predominate in the middle and lower parts of Unit 3 where the 'redbed' facies is commonly interbedded with the 'ribboned' facies (Southgate, 1991). The upper parts of Unit 3 in Wallara 1 consist of shallower water facies, namely the 'thinly-bedded and 'redbed' facies of Southgate (1991). Unit 3 in Wallara 1 culminates in quartz sandstone and minor siltstone facies, which are not seen in outcrop. This is consistent with the stratigraphy at locality 1. Sandstone–siltstone–dolomite facies continue into the Johnnys Creek beds but there is abundant green siltstone in the Johnnys Creek beds that was presumably deposited below wave base.

The $\delta^{18}O$ values, apart from the uppermost two values that are similar to those from dolomite in the Johnnys Creek beds, are more

Table 1
Isotope analyses and locations of carbonate samples from units atop the Bitter Springs Formation, northeastern Amadeus Basin, Australia

Sample no.	δ^{18}OPDB	δ^{13}CPDB	Latitude	Longitude	UTM (N)	UTM (E)
Ellery Creek						
Bitter Springs						
EC2c	−7.89	6.01	23 46.94′S	133 01.61′E		
EC3c	−4.89	5.34	23 46.94′S	133 01.61′E		
EC5c	−8.52	6.34	23 46.94′S	133 01.61′E		
EC8c	−6.18	4.12	23 46.94′S	133 01.61′E		
EC9c	−8.69	5.58	23 46.94′S	133 01.61′E		
EC12c	−10.35	4.00	23 46.94′S	133 01.61′E		
EC13c	−5.63	4.28	23 46.94′S	133 01.61′E		
EC16c	−3.99	−2.26	23 46.94′S	133 01.61′E		
Upper interbedded dolomite beds at Ellery Creek						
EC19c	−4.21	1.04	23 46.94′S	133 01.61′E		
EC20c	−3.40	0.82	23 46.94′S	133 01.61′E		
EC21c	−4.04	0.42	23 46.94′S	133 01.61′E		
EC23c	−5.39	2.27	23 46.94′S	133 01.61′E		
EC27c	−4.18	1.61	23 46.94′S	133 01.61′E		
Ross River						
Cap dolomite						
RR1c	−8.48	1.20	23 35.15′S	134 29.48′E	7391560N	53448090E
RR2	−7.93	2.71	23 35.15′S	134 29.48′E	7391560N	53448090E
RR3	−7.91	2.82	23 35.15′S	134 29.48′E	7391560N	53448090E
RR4	−8.41	2.79	23 35.15′S	134 29.48′E	7391560N	53448090E
RR5c	−3.49	2.47	23 35.15′S	134 29.48′E	7391560N	53448090E
RR7c	−7.24	0.51	23 35.15′S	134 29.48′E	7391560N	53448090E
RR8c	−4.36	2.54	23 35.15′S	134 29.48′E	7391560N	53448090E
RR9c	−5.91	2.01	23 35.15′S	134 29.48′E	7391560N	53448090E
Bitter Springs						
RR25c	−4.80	1.98	23 35.15′S	134 29.48′E	7391560N	53448090E
RR26c	−4.84	2.03	23 35.15′S	134 29.48′E	7391560N	53448090E
RR27c	−7.93	3.04	23 35.15′S	134 29.48′E	7391560N	53448090E
RR28c	−8.51	3.58	23 35.15′S	134 29.48′E	7391560N	53448090E
RR29c	−8.32	3.02	23 35.15′S	134 29.48′E	7391560N	53448090E
RR30c	−8.65	4.01	23 35.15′S	134 29.48′E	7391560N	53448090E
RR31c	−5.94	3.66	23 35.15′S	134 29.48′E	7391560N	53448090E
Corroboree Rock						
Cap dolomite						
CR4	−9.60	−1.13	23 42.20′S	134 13.85′E	7378500N	53421550E
CR14	−10.01	−1.06	23 41.80′S	134 13.70′E	7379200N	53421500E
CR19	−8.54	−2.82	23 41.70′S	134 13.70′E	7379250N	53421400E
Pebbly cap dolomite						
CR1	−7.02	−1.55	23 42.50′S	134 14.35′E	7377800N	53422450E
CR2	−7.59	−2.21	23 42.50′S	134 14.35′E	7377800N	53422450E
Breccia clasts and matrix						
F1 (micrite)	−2.86	3.50	23 42.20′S	134 13.85′E	7378500N	53421500E
F2 (micrite)	−2.88	3.70	23 42.20′S	134 13.85′E	7378500N	53421500E
F3 (micrite)	−2.33	4.00	23 42.20′S	134 13.85′E	7378500N	53421500E
F4 (micrite)	−2.49	4.30	23 42.20′S	134 13.85′E	7378500N	53421500E
F5 (micrite)	−3.37	3.70	23 42.20′S	134 13.85′E	7378500N	53421500E
F6 (micrite)	−3.24	3.22	23 42.20′S	134 13.85′E	7378500N	53421500E
F1 (spar)	−9.52	2.67	23 42.20′S	134 13.85′E	7378500N	53421500E
F2 (spar)	−8.02	2.39	23 42.20′S	134 13.85′E	7378500N	53421500E
F5 (spar)	−3.1	3.50	23 42.20′S	134 13.85′E	7378500N	53421500E
M1 (matrix)	−5.69	−1.68	23 42.20′S	134 13.85′E	7378500N	53421500E
M3 (matrix)	−5.06	−3.68	23 42.20′S	134 13.85′E	7378500N	53421500E
Bitter Springs						
CR6c	−5.18	2.67	23 41.90′S	134 13.70′E	7379100N	53421400E
CR7c	−4.93	4.35	23 41.90′S	134 13.70′E	7379100N	53421400E
CR8c	−6.07	3.86	23 41.90′S	134 13.70′E	7379100N	53421400E
CR9c	−8.19	3.80	23 41.90′S	134 13.70′E	7379100N	53421400E
CR10c	−9.56	3.07	23 41.90′S	134 13.70′E	7379100N	53421400E
CR11c	−10.03	−0.24	23 41.90′S	134 13.70′E	7379100N	53421400E
CR12c	−3.23	2.11	23 41.90′S	134 13.70′E	7379100N	53421400E
CR13c	−3.10	2.04	23 41.90′S	134 13.70′E	7379100N	53421400E
No. of Gaylad Syncline						
Dolomite at top of Bitter Springs between boxwork chert veins						
9.12.03-6	−8.05	−1.92	23 40.20′S	134 50.43′E	7379000N	53491000E
9.12.03-7	−8.48	−0.41	23 40.20′S	134 50.43′E	7379000N	53491000E
9.17.03-11	−4.12	−1.97	23 40.20′S	134 50.43′E	7379000N	53491000E

Table 1 (*Continued*)

Sample no.	δ^{18}OPDB	δ^{13}CPDB	Latitude	Longitude	UTM (N)	UTM (E)
9.17.03-12	−5.3	−1.96	23 40.20′S	134 50.43′E	7379000N	53491000E
9.17.03-19	−5.3	−2.03	23 40.20′S	134 50.43′E	7379000N	53491000E
9.12.03-24	−4.91	−3.11	23 40.20′S	134 50.43′E	7379000N	53491000E
9.17.03-29	−4.1	0.323	23 40.20′S	134 50.43′E	7379000N	53491000E
Along road N. of Corroboree Rock						
Cap dolomite						
R-20	−8.99	0.75	23 41.28′S	134 14.35′E	7380101N	53422434E
R-21c	−5.24	2.61	23 41.28′S	134 14.35′E	7380101N	53422434E
R-23	−4.73	1.28	23 41.28′S	134 14.35′E	7380101N	53422434E
R-24	−4.84	−0.086	23 41.28′S	134 14.35′E	7380101N	53422434E
Hidden Valley						
Cap dolomite						
HV-4	−9.31	−0.66	23 39.94′S	134 15.09′E	7382585N	53423682E
HV-5	−8.07	0.41	23 39.94′S	134 15.09′E	7382585N	53423682E
HV-6	−9.12	0.025	23 39.94′S	134 15.09′E	7382585N	53423682E

depleted (by up to a 2–3‰) in ^{18}O than in Wallara 1, and in the lower parts of Unit 3 of the BSF exposed in drillholes AS 27 and AS 28 (Hill et al., 2000). This could be attributed to regional differences (including different diagenetic environments) to which δ^{18}O is sensitive.

5.3.1.2. Breccia clasts and matrix. The fenestrate micrite clasts (samples F2 to F6) are isotopically homogenous, with δ^{13}C values within ±0.5‰ of each other and similar (3.2–4.3‰) to those in the uppermost BSF (2.7–4.4‰) as shown in Fig. 5. δ^{18}O values in the breccia clasts (−3.4 to −2.3‰) are heavier than those in the uppermost BSF (−6.0 to −4.9‰). Kennedy et al. (2001) reported δ^{13}C values from 'fenestral and non-fenestral' dolomites of the Olympic Formation of between −0.1 and +3.6‰, with an average of +1.8‰. Therefore, it is unlikely that the fenestrate or non-fenestrate breccia clasts are from the Olympic Formation, which is consistent with the sedimentological data.

The fenestrae spar δ^{13}C values are between 0 and 1‰ lighter than the fenestrate micrite clasts and two fenestrae spar δ^{18}O values (samples F1 and F2) are 5–6‰ lighter than the fenestrate micrite, but similar to some BSF values. The co-occurrence of lighter δ^{13}C and δ^{18}O values and spar-sized crystals is consistent with later diagenetic crystal growth in solutions mixed with re-dissolved micrite and isotopically depleted (much more in δ^{18}O than δ^{13}C) because meteoric water has very low dissolved inorganic carbon concentrations (Land, 1992) meteoric waters. The lighter δ^{13}C and δ^{18}O values in fenestral spar are similar to those from 'fenestral' and 'non-fenestral' dolomites of the Olympic Formation (Kennedy et al., 2001), however, sedimentological analysis suggests that this is unlikely.

δ^{13}C values of the dolomicritic matrix are 4–8‰ lighter than the breccia clasts and similar to values from the overlying cap dolomite, and to previously reported values for cap dolomite in the northeastern Amadeus Basin (range, −0.5 to −8.4‰; average, ∼−3‰; Kennedy, 1996; Kennedy et al., 2001).

Based on the isotopic data the breccia clasts were probably derived from the underlying BSF and the matrix precipitated directly from ambient seawater which was ^{13}C-depleted at the time δ^{13}C (values on average between −5 and 0‰), relative to the BSF. In the Amadeus Basin, between deposition of the BSF and the Pertatataka Formation, there are only two known times when seawater δ^{13}C was this depleted, and they were immediately after the Sturtian glacial epoch (in the lowermost Aralka Formation; Walter et al., 2000) and in the 'cap dolomite' that rests on the upper erosional surface of the Pioneer Formation (Calver, 1995; Kennedy, 1996; Kennedy et al., 2001). The δ^{13}C record of the Adelaide Rift Complex also has negative δ^{13}C values in carbonates immediately after the Sturtian (McKirdy et al., 2001) and Marinoan (Calver, 2000) glacial epochs. Negative values are also found in the Trezona Formation just under the Marinoan Elatina Formation, however, the δ^{13}C carb values in the Trezona Formation fall mostly between −10 and −4‰ (McKirdy et al., 2001) which are more ^{13}C-depleted than the matrix values presented here. The co-occurrence of the breccia with sandstone and conglomerate of the Pioneer Sandstone and similarly ^{13}C-depleted values in the cap dolomite (Fig. 5) suggests precipitation of the breccia matrix after the Marinoan glacial epoch, rather than after the Sturtian glacial epoch.

5.3.1.3. Cap dolomite. The δ^{13}C and δ^{18}O values (including samples CR1 and CR2 from locality 2) are comparable to those of Kennedy (1996) and Kennedy et al. (2001), and other Marinoan cap dolomites in Australia (Kennedy, 1996; Calver, 2000) and worldwide (Halverson et al., 2005).

5.3.1.4. Along road north and east of Corroboree Rock. The ∼2 m dolomite breccia bed northeast of Corroboree Rock has a similar isotopic composition to the dolomite breccia and underlying BSF at locality 1 (Fig. 5) suggesting a common origin.

5.3.2. Ross River data

5.3.2.1. Bitter Springs Formation. The δ^{13}C and δ^{18}O values compare with the Corroboree Rock data and are indicative of the uppermost parts of Unit 3 of the Loves Creek Member.

5.3.2.2. Cap dolomite. The δ^{13}C and δ^{18}O values are not consistent with the cap dolomite to the Pioneer Sandstone, and it is not BSF. The isotope data are comparable to those reported from dolomite beds within the Olympic Formation (Kennedy et al., 2001), therefore the simplest explanation is that this is not the 'cap dolomite' but the Olympic Formation. Field (1991) described all these three rock types (pebbly sandstone and conglomerate, breccia, and dolomite beds) within the Olympic Formation at the same stratigraphic position, and Lindsay (1989) stated that the only known exposures of the Olympic Formation are in the Ooraminna sub-basin in the northeastern Amadeus Basin.

It is possible that the sandstone beds beneath the breccia and 'cap dolomite' may be part of the Undoolya sequence (Kennedy, 1993), in which case the dolomite bed may be part of the lower Pertatataka Formation. However, this does not seem likely considering all exposures of the lower Pertatataka Formation in the region are composed of dark shales and that δ^{13}C values from interbeds of limestone in the lower Pertatataka Formation are between −2.9

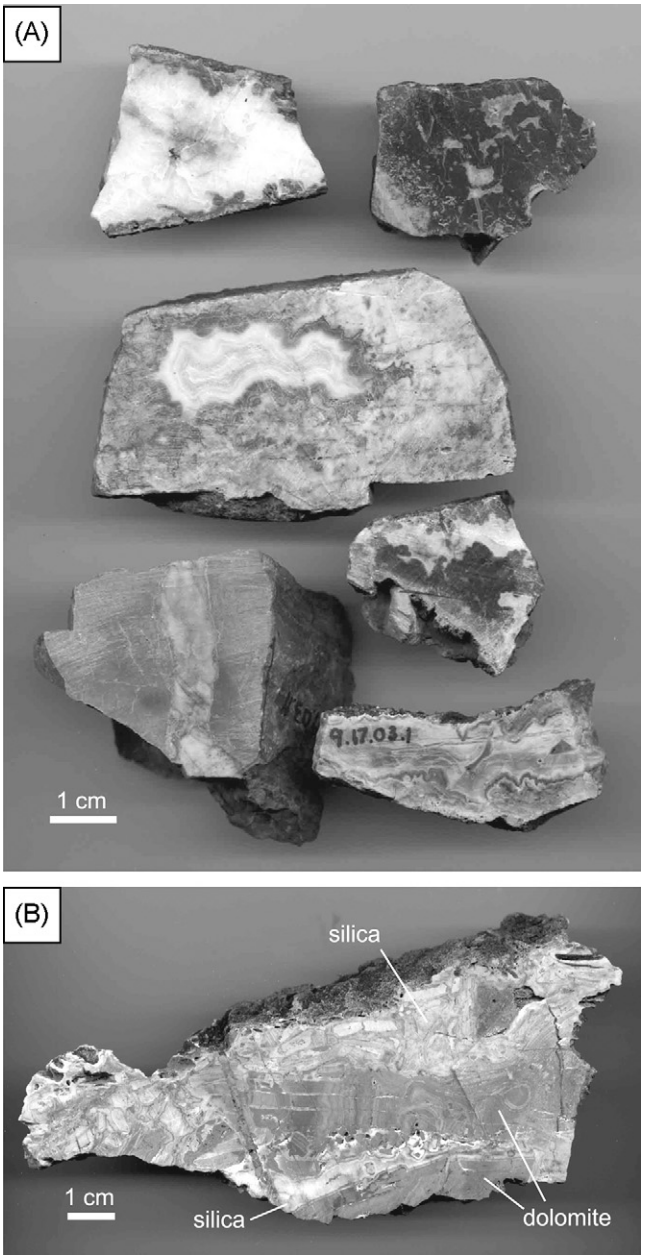

Fig. 13. Cut slabs of secondary silica from the top of the Bitter Springs Formation on the north side of the Gaylad Syncline. (A) Light gray to white silica fills former cavities in dark gray to black early diagenetic Bitter Springs cherts. Former cavities are lined with botryoidal chalcedony and the centre of the cavities are filled with coarse megaquartz. (B) Gray Bitter Springs dolomite, showing contorted bedding, is cut by dissolution cavities lined with light gray botryoidal chalcedony and filled with coarse megaquartz.

and 0.9‰ (Kennedy et al., 2001). It is also possible that this dolomite bed represents the last remnant of a previously unobserved formation that was nearly completely stripped prior to deposition of the Pioneer Sandstone. However, this would invoke yet another erosional hiatus within Supersequence 4, which also seems unlikely considering such a hiatus has not been recognized anywhere else in the region.

5.3.3. Ellery Creek data

5.3.3.1. Bitter Springs Formation. The $\delta^{13}C$ values, which are between +4 and +6‰ (apart from sample EC16c), are indicative of the lower and middle parts of Unit 3 of the Loves Creek Member where the 'ribboned' and 'redbed' facies of Southgate (1991) are interbedded (Hill et al., 2000). Therefore, the uppermost parts of Unit 3 that are present near Corroboree Rock and Ross River are not preserved at Ellery Creek.

5.3.3.2. Upper interbedded dolomite beds. These strata directly overlie the BSF at Ellery Creek, are over 40 m thick, and contain mostly quartz sandstones interbedded with minor, very thin laminated dolomite. These dolomite beds have similar isotopic values to those of the dolomite at Ross River and northeast of Corroboree Rock, but not to those of the cap dolomites at Corroboree Rock and elsewhere in Australia. It is not clear to which named unit these beds belong, however, as discussed above, the lithologies and isotopic data are consistent with those of the Olympic Formation. It is also possible that lateral equivalents far west of the type locality of the Pioneer Sandstone do indeed contain thin beds of dolomite, or that these beds are a distal facies of the Areyonga Formation or a formation not previously recognized, but the simplest explanation is that they are part of the Olympic Formation.

5.3.4. Hidden Valley

The $\delta^{13}C$ and $\delta^{18}O$ values for samples HV-4, HV-5 and HV-6 are typical of other cap dolomite values in the northeastern Amadeus Basin (this paper; Calver, 1995; Kennedy, 1996; Kennedy et al., 2001), and their stratigraphic position below the Elleria minuta stromatolite bed supports a cap dolomite origin.

5.4. Discussion of the Bitter Springs volcanics

Previous workers have noted the presence of mafic, apparently volcanic rocks within portions of the BSF (Wells et al., 1967; Shaw and Wells, 1983). There is some ambiguity as to whether these rocks represent volcanic flows or intrusive sills. If they are flows, then they are coeval with deposition of the BSF. If they are sills, they may be coeval or much younger. Although volumetrically minor, these rocks are apparently widespread throughout the Amadeus Basin (Shaw et al., 1991), and occur in both drill holes and outcrops (Zhao et al., 1994).

During this study mafic rocks within the BSF were observed in two different localities in the northeastern Amadeus Basin. North of Corroboree Rock, in the strike-valley partly filled by the Undoolya sequence (Kennedy, 1993), mafic rock occurs in small, poorly exposed pods several meters long and up to ~1 m or so thick along the contact with the BSF and the overlying brown sandstone and siltstone of the overlying Undoolya sequence. The mafic rock crumbles easily but light gray plagioclase laths up to 5 mm long are relatively fresh. Kennedy (1993) observed these same outcrops (up to 20 m long). He interpreted them as intrusions in the BSF and possibly in the Undoolya sequence as well, but was not certain if the mafic rocks were restricted to the contact or were slightly above it (M. Kennedy, personal communication, 2004). Their lens-like shape apparently restricted to the contact suggests these outcrops may represent the remnants of weathered flows, but they could also be sills.

At the Ross River locality (see Fig. 9), immediately uphill from a black chert horizon (Barghoorn and Schopf, 1965), a recessively weathering layer of dark gray-green mafic rock up to 20 m thick separates dolomite beds of the Loves Creek Member of the BSF. The mafic rock shows no internal layering or obvious vesicles or amygdales. The lower contact is mostly covered by slope debris, but the upper contact is exposed locally and in at least one place is discordant to bedding in the overlying dolomite. Laterally along the contact, the mafic rock is conformable then bulges upward several meters into a gray, cliff-forming dolomite bed over a lateral

span of about 5 m. The contact appears sharp and the dolomite bed appears slightly bowed upward as well. The discordancy of the contact and the absence of recognizable vesicles or amygdales suggests this exposure is likely a mafic sill that intruded well up into the Loves Creek Member.

Walter and Veevers (1997) noted that there are mafic sills of similar composition within the Jillyili and Coondra Formations in the Savory Sub-basin of the western Officer Basin of comparable age to the BSF. The εNd values of the BSF mafic rocks are similar to those in the Amata dike swarm, dated at ~800 Ma (Sm–Nd isochron, Zhao et al., 1994), that intrude older granitic and metamorphic rocks of the Musgrave block. The trace-element distribution in the BSF mafic rocks is also similar to the Amata dikes, as well as similar to the Wooltana (Willouran) volcanics in the Adelaide Basin, and although, by superposition, the BSF mafic rocks are younger than the Amata dikes, it is possible they all tapped a common igneous source (Zhao et al., 1994).

6. Conclusions

The quartz sandstone and chert-carbonate-clast conglomerate at Corroboree Rock and at Ross River are likely part of the Pioneer Sandstone, based on lithology, stratigraphic position, and the existence of a basal angular unconformity at Corroboree Rock. C and O isotopic values of sedimentary carbonate indicate that the laminoid fenestrate breccia deposits were probably derived from the underlying BSF, even though fenestrate rocks of this type are not seen in outcrop. Isotopic values of the chert-bearing dolomite above the Pioneer Sandstone at Ross River, and the interbedded sandstone and thin dolomite beds at Ellery Creek, suggest they are part of the Olympic Formation, or, less likely, a previously unknown formation.

C and O isotopic values of the 1–2 m-thick pink dolomite and dolomite breccia between Corroboree Rock and Hidden Valley are consistent with values of other "cap carbonates" in Australia. The presence of brecciated textures within the dolomite can be explained by strong wave action (storm or tsunami?) in relatively shallow water, and suggests a shallow-water origin for these deposits. The presence of the very thin, 10–20 cm-thick layer of Elleria minuta stromatolites everywhere at the top of the pink dolomite and immediately below the purple shales of the Pertatataka Formation is a very useful marker horizon and indicates very stable conditions. The coarse quartz sand filling the interspaces between stromatolites, however, suggests exposure and erosion of the underlying metamorphic basement or the Heavitree Quartzite, and transport of that sand over a very short time interval. The cause of that transport is unknown. Time and funding constraints did not allow for an examination of the C and O isotopic composition of cherts within the Bitter Springs Formation, the varicolored cherts in the uppermost dolomite bed at Ross River, and within the box-work silica veins at the top of the Bitter Springs Formation in the Gaylad syncline. A study of these cherts would help to determine the diagenetic histories of these deposits.

Acknowledgements

This project was partially supported by a grant to SJS from the NASA Astrobiology Institute (NAI) as a Post-doc position at the Australian Centre for Astrobiology (ACA) at Macquarie University in Sydney, Australia. Our thanks go to Paul Knauth for support of the isotope analyses and use of his mass spectrometer at Arizona State University. This is a contribution to IGCP project 512: Neoproterozoic Ice Ages (www.IGCP512.com).

References

Barghoorn, E.S., Schopf, J.W., 1965. Microorganisms from the late Precambrian of central Australia. Science 150, 337–339.
Black, L.P., Shaw, R.D., Offe, L.A., 1980. The age of the Stuart dyke swarm and its bearing on the onset of late Precambrian sedimentation in central Arizona. Journal of the Geological Society of Australia 27, 151–155.
Calver, C.R., 1995. Ediacarian isotope stratigraphy of Australia. Ph.D. Thesis. Macquarie University, Sydney, Australia.
Calver, C.R., 2000. Isotope stratigraphy of the Ediacarian (Neoproterozoic III) of the Adelaide Rift Complex, South Australia, and the overprint of water column stratification. Precambrian Research 100, 121–150.
Coats, R.P., Preiss, W.V., 1980. Stratigraphic and geochronological reinterpretation of Lte Proterozoic glaciogenic sequences in the Kimberley Region, Western Australia. Precambrian Research 13, 181–208.
Ding, P., James, P.R., Sandiford, M., 1992. Late Proterozoic deformation in the Amadeus Basin, central Australia. Australian Journal of Earth Sciences 39, 495–500.
Field, B.D., 1991. Paralic and periglacial facies and contemporaneous deformation of the late Proterozoic Olympic Formation, Pioneer Sandstone, and Gaylad Sandstone, Amadeus Basin, central Australia. Bureau of Mineral Resources Geological and Geophysical Bulletin 236, 127–136.
Forman, D.J., 1966. Bloods Range, Northern Territory, 1:250,000 Geological Series. Bureau of Mineral Resources, Australia, Explanatory Notes, Sheet SG/52-3.
Freeman, M.J., Oaks Jr., R.Q., Shaw, R.D., 1991. Stratigraphy of the late Proterozoic Gaylad Sandstone, northeastern Amadeus Basin, and recognition of an underlying regional unconformity. Bureau of Mineral Resources Geological and Geophysical Bulletin 236, 137–154.
Froelich, A.J., Krieg, E.A., 1969. Geophysical-geologic study of the northern Amadeus Trough, Australia. Bulletin of the American Association of Petroleum Geologists 53, 1978–2004.
Glikson, A.Y., Stewart, A.J., Ballhaus, C.G., Clarke, G.L., Feeken, E.H.J., Sheraton, J.W., Sun, S.-S., 1996. Geology of the western Musgrave Block, central Australia, with particular reference to the mafic–ultramafic Giles Complex. Australian Geological Survey Organization Bulletin 239, 41–68.
Grey, K., Hocking, R.M., Stevens, M.K., Bagas, L., Carlsen, G.M., Irimies, F., Pirajno, F., Haines, P.W., Apak, S.N., 2005. Lithostratigraphic nomenclature of the Officer Basin and correlative parts of the Paterson Orogen, Western Australia. Western Australia Geological Survey. Report 93.
Grotzinger, J.P., 1986. Evolution of early Proterozoic passive-margin carbonate platform, Rocknest Formation, Wopmay orogen, Northwest Territories, Canada. Journal of Sedimentary Petrology 56 (6), 831–847.
Halverson, G.P., Hoffman, P., Schrag, D.P., Maloof, A.C., Rice, A., 2005. Towards a Neoproterozoic composite carbon isotope record. Geological Society of America Bulletin 117, 1181–1207.
Hill, A.C., Walter, M.R., 2000. Mid-Neoproterozoic (~830–750 Ma) isotope stratigraphy of Australia and global correlation. Precambrian Research 100, 181–211.
Hill, A.C., Arouri, K., Gorjan, P., Walter, M.R., 2000. Geochemistry of marine and nonmarine environments of a Neoproterozoic cratonic carbonate/evaporite; the Bitter Springs Formation, central Australia. In: Grotzinger, J.P., Noel, J.P. (Eds.), Carbonate Sedimentation and Diagenesis in the Evolving Precambrian World, vol. 67. Society of Economic Paleontologists and Mineralogists (SEPM) Special Publication, pp. 327–344.
Hill, C., Forti, P., 1997. Cave Minerals of the World. National Speleological Society Inc.
Horodyski, R.J., Knauth, L.P., 1994. Life on land in the Precambrian. Science 263 (5146), 494–498.
Kennard, J.M., Lindsay, J.F., 1991. Sequence stratigraphy of the latest Proterozoic. Cambrian Pertaoorrta Group, northern Amadeus Basin, central Australia. In: Korsch, R.J., Kennard, J.M. (Eds.), Geological and Geophysical Studies in the Amadeus Basin, Central Australia. Bureau of Mineral Resources, Australia. Bulletin 236, 171–194.
Kennedy, M.J., 1993. The Undoolya Sequence; Late Proterozoic salt influenced deposition, Amadeus Basin, Australia. Australian Journal of Earth Sciences 40, 217–228.
Kennedy, M.J., 1996. Stratigraphy, sedimentology, and isotopic geochemistry of Australian Neoporoterozoic postglacial cap dolostones; deglaciation, $\delta^{13}C$ excursions, and carbonate precipitation. Journal of Sedimentary Research 66 (6), 1050–1064.
Kennedy, M.J., Christie-Blick, N., Prave, A.R., 2001. Carbon isotopic composition of Neoproterozoic glacial carbonates as a test of paleoceanographic models for snowball Earth phenomena. Geology 29 (12), 1135–1138.
Knoll, A.H., Walter, M.R., 1992. Latest Proterozoic stratigraphy and Earth history. Nature 356, 673–678.
Land, L.S., 1992. The dolomite problem: stable and radiogenic isotope clues. In: Clauer, N., Chaudhuri, S. (Eds.), Isotopic Signatures and Sedimentary Records: Lecture Notes in Earth Sciences, vol. 43. Springer-Verlag, New York, pp. 49–68.
Lindsay, J.F., 1987. Upper Proterozoic evaporites in the Amadeus Basin, central Australia, and their role in basin tectonics. Geological Society of America Bulletin 99, 852–865.
Lindsay, J.F., 1999. Heavitree Quartzite, a Neoproterozoic (ca 800–760 Ma) high-energy, tidally influenced, ramp association, Amadeus Basin, central Australia. Australian Journal of Earth Sciences 46, 127–139.
Lindsay, J.F., 1989. Depositional controls on glacial facies associations in the basinal setting, late Proterozoic, Amadeus Basin, central Australia. Palaeogeography, Palaeoclimatology, Palaeoecology 73, 205–233.

McKirdy, D.M., Burgess, J.M., Lemon, N.M., Yu, X., Cooper, A.M., Gostin, V.A., Jenkins, R.J.F., Both, R.A., 2001. A chemostratigraphic overview of the late Cryogenian interglacial sequence in the Adelaide Fold-Thrust Belt, South Australia. Precambrian Research 106, 149–186.

Morton, J.G.G., 1997. Lithostratigraphy and environments of deposition (Chapter 6). In: Morton, J.G.G., Drexel, J.F. (Eds.), Petroleum Geology of South Australia, vol. 3. Officer Basin, South Australia Department of Mines and Energy Resources Report Book 97/19.

Preiss, W.V., 1987. The Adelaide Geosyncline—late Proterozoic stratigraphy, sedimentation, paleontology and tectonics. South Australian Geological Survey Bulletin 53, 438.

Preiss, W.V., Forbes, B.G., 1981. Stratigraphic correlation and sedimentary history of Adelainian (Late Proterozoic) basins in Australia. Precambrian Research 15, 255–304.

Preiss, W.V., Walter, M.R., Coats, R.P., Wells, A.T., 1978. Lithologic correlations of Adelaidean glaciogenic rocks in parts of the Amadeus, Ngalia, and Georgina Basins. Bureau of Mineral Resources Journal of Australian Geology and Geophysics 3, 45–53.

Schopf, J.W., 1968. Microflora of the Bitter Springs Formation, late Precambrian, central Australia. American Association of Petroleum Geologists Bulletin 42 (3), 651–689.

Shaw, R.D., Wells, A.T., 1983. Alice Springs, Northern territory, 1:250,000 Geological Series. Bureau of Mineral Resources, Australia, Explanatory Notes, Sheet SF/53-14 (second edition).

Shaw, R.D., Etheridge, M.A., Lambeck, K., 1991. Development of the late Proterozoic tomid-Paleozoic, intercratonic Amadeus Basin in central Australia; a key to understanding tectonic forces in plate interiors. Tectonics 10 (4), 688–721.

Shaw, R.D., Langworthy, A.P., Stewart, A.J., Offe, L.A., Jones, B.G., O'Donnell, I.C., Knight, C.P., 1983. Alice Springs, Northern Territory 1:250,000 Geological Series, 2nd ed. Australian Bureau of Mineral Resources, Geology and Geophysics (Geologic Map, SF53-14).

Southgate, P.N., 1991. A sedimentological model for the Loves Creek Member of the Bitter Springs Formation, northern Amadeus Basin. Bureau of Mineral Resources Geological and Geophysical Bulletin 236, 113–126.

Tebbutt, G., Conley, C., Boyd, D., 1965. Lithogenesis of a distinctive carbonate rock fabric. Contributions to Geology 4 (1), 1–13.

Walter, M.R., 1972. Stromatolites and the biostratigraphy of the Australian Precambrian and Cambrian. Special paper of the paleontological Association of London 1, 190.

Walter, M.R., Krylov, I.N., Preiss, W.V., 1979. Stromatolites from Adelaidean (late Proterozoic) sequences in central and South Australia. Alcheringa 3, 287–305.

Walter, M.R., Veevers, J.J., 1997. Australian Neoproterozoic palaeogeography, tectonics, and supercontinental connections. AGSO Journal of Australian Geology and Geophysics 17 (1), 73–92.

Walter, M.R., Veevers, J.J., Calver, C.R., Gorjan, P., Hill, A.C., 2000. Dating the 840–544 Ma Neoproterozoic interval by isotopes of strontium, carbon, and sulfur in seawater, and some interpretive models. Precambrian Research 100, 371–433.

Walter, M.R., Veevers, J.J., Calver, C.R., Grey, K., 1995. Neoproterozoic stratigraphy of the Centralian Superbasin, Australia. Precambrian Research 73, 173–195.

Wells, A.T., Ranford, L.C., Stewart, A.J., Cook, P.J., Shaw, R.D., 1967. The geology of the northeastern part of the Amadeus Basin. Northern Territory, Bureau of Mineral Resources, Australia. Report 113, 93.

Wells, A.T., Forman, D.J., Ranford, L.C., Cook, P.J., 1970. Geology of the Amadeus Basin, central Australia, Bureau of Mineral Resources, Australia. Bulletin 100, 222.

Williams, G.E., Jenkins, R.J.F., Walter, M.R., 2007. No heliotropism in Neoproterozoic columnar stromatolite growth, Amadeus Basin, central Australia, Geophysical implications. Palaeogeography, Palaeoclimatology, Palaeoecology 249 (1/2), 80–89.

Wingate, M.T.D., Campbell, I.H., Compston, W., Gibson, G.M., 1998. Ion microprobe U–Pb ages for Neoproterozoic basaltic magmatism in south-central Australia and implications for the breakup of Rodinia. Precambrian Research 87, 135–159.

Wingate, M.T.D., Pirajno, F., Morris, P.A., 2004. Warakurna large igneous province; a new Mesoproterozoic large igneous province in west-central Australia. Geology 32 (2), 105–108.

Zhao, J.-X., McCulloch, M.T., Korsch, R.J., 1994. Characterization of a plume-related ~800 Ma magmatic event and its implications for basin formation in central-southern Australia. Earth and Planetary Science Letters 121, 349–367.